1-1-2021

DEVELOPMENT OF SITE - SPECIFIC DRUG DELIVERY SYSTEMS USING HOT MELT EXTRUSION AND FUSED DEPOSITION MODELING 3D PRINTING

NAGIREDDY REDDY DUMPA
University of Mississippi

DEVELOPMENT OF SITE - SPECIFIC DRUG DELIVERY SYSTEMS USING HOT MELT EXTRUSION AND FUSED DEPOSITION MODELING 3D PRINTING

A Dissertation Submitted

In the Partial Fulfillment of the Requirements For

The Doctor of Philosophy Degree in Pharmaceutical Sciences

With an emphasis in Pharmaceutics and Drug Delivery

The University of Mississippi

By

NAGIREDDY DUMPA

ABSTRACT

Due to preferential site of drug absorption and need for increased concentration of medication at the required tissues, dosage forms should be designed or formulated in such way that medication is released at specific site or after specific time in the gastrointestinal tract (GIT). Knowledge of transit times of dosage forms in each part of GIT, by use of particular polymers or employing specific delivery systems such as floating systems, delivery of medication to specific sites in the GIT can be achieved. HME coupled FDM 3D printing has capability to create customized dosage forms for personalized pharmacotherapy with its ability to produce dosage forms with complex structures, customized shapes, and sizes. Chronotherapy deals with synchronizing drug delivery with the body's circadian rhythm to optimize therapeutic efficacy and minimize side effects. Using the advantage of pH dependent solubility of Eudragit S100 (ES100) (as an enteric polymer that solubilizes and releases the drug at above pH 7), a chronotherapeutic drug delivery system for KTP and IBU was successfully developed for the treatment of arthritis conditions in the early morning hours. The drug release studies conducted in different media showed the desired lag time and release characteristics. Maintaining a constant plasma drug concentration is not beneficial in all disease conditions. Some diseases may require pulse delivery of drugs to avoid unwanted adverse effects and drug exposure. Various biological factors influence the transit time of drugs in the upper gastrointestinal tract and possess a challenge to the drugs that are locally active in the stomach, unstable at a high pH, or poorly soluble in the lower parts of the gastrointestinal tract. To overcome these issues, a floating pulsatile system was developed which

showed a high potential to deliver drugs that need high residence time in the stomach and the pulsatile release of theophylline. Quality by design (QbD) is defined as a systematic approach to development that begins with predefined objectives and emphasizes product and process understanding based on sound science and quality risk management. QbD is combined with FDM 3D printing to develop personalized dosage forms for patient centric pharmacotherapy.

DEDICATION

This work is dedicated to my family, teachers, and friends for their continuous support and belief in me.

LIST OF ABBREVIATIONS AND SYMBOLS

HME – Hot melt extrusion

FDM – Fused deposition modeling

GIT – Gastrointestinal tract

KTP –Ketoprofen

IBU – Ibuprofen

HPC – Hydroxypropyl cellulose

EC – Ethyl cellulose

ES100 – Eudragit S100

API – Active Pharmaceutical ingredient

Tg – Glass transition

HPMC – Hydroxy propyl methyl cellulose

ºC – Degrees centigrade

RPM – Rotations per minute

ºC – Degrees centigrade

RPM – Rotations per minute

PSD – Particle size distribution

%w/w – weight / weight

%w – Percentage weight

%v/v – volume/volume

Min – Minutes

g- Gram

mg- Milligram

Kg – Kilogram

L – Liter

h- Hour

mL - Milliliter

µ- Micron

µM – Micrometer

µL – Microliter

cm – Centimeter

mm- Millimeter

nm – Nanometer

s – second

kV- Kilovolts

mA – Milli amperes

HPLC – High performance liquid chromatography

UV – Ultraviolet

VIS – Visible

FTIR - Fourier-transform infrared spectroscopy

DSC – Differential scanning calorimetry

XRD – X- ray powder diffraction

PXRD - Powder X- ray powder diffraction

HCl – Hydrochloric acid

NaOH – Sodium Hydroxide

HDPE – High density polyethylene

ANOVA – Analysis of variance

Nm – Newton-meter

KP- Kilopond

3D – Three dimensional

SEM - Scanning electron microscopy

ACKNOWLEDGEMENTS

Research Advisor:

Dr. Michael A. Repka (Dept. of Pharmaceutics and Drug Delivery)

Committee Members

Dr. S. Narasimha Murthy (Dept. of Pharmaceutics and Drug Delivery)

Dr. Seongbong Jo (Dept. of Pharmaceutics and Drug Delivery)

Dr. Samir A. Ross (Dept. of Biomolecular sciences)

Faculty Members in the department of Pharmaceutics and Drug Delivery

Dr. Suresh Bandari

Ms. Deborah

All the students in Dr. Repka's group and in the department

Friends and room mates

Family Members

TABLE OF CONTENTS

LIST OF TABLES

LIST OF FIGURES

CHAPTER 1
INTRODUCTION

1.1 Introduction to site specific drug delivery systems

Oral route is the most convenient and preferred route for administration of dosage forms because of advantages associated with it such as ease of administration, flexibility in dosing, low cost, and high availability. But however due to preferential site of drug absorption and need for increased concentration of medication at the required tissues, dosage forms should be designed or formulated in such way that medication is released at specific site or after specific time in the gastrointestinal tract (GIT). Various researchers developed different drug delivery systems aiming at different parts of the GIT including mouth, stomach, small intestine, and colon (J. F pinto et al., 2010; T. Bussemer et al., 2001). For example, medications intended for ulcerative colitis, crohn's disease, colonic cancer, and chronotherapeutic conditions dosage forms need to be delivered to the lower part of the gastrointestinal tract for improved treatment efficacy and minimal side effects. Whereas for drugs that are locally active in the stomach, unstable at high pH or that have poor solubility in lower parts of the colon, there is need for increased residence time in stomach or upper parts of the GIT (S. Das et al.; 2010; J. Worsoe et al., 2011; A. Streubel et al., 2006). Knowledge of transit times of dosage forms in each part of GIT, by use of particular polymers or employing specific delivery systems such as floating systems, delivery of medication to specific sites in the GIT can be achieved (F. Siepmann et al., 2008).

1.2 Hot melt extrusion in Pharmaceutics and drug delivery

Hot-melt extrusion (HME) is a well-known technique used in the plastic, rubber, and food industries but over the last three decades HME technology has gained significant attention in pharmaceutical research and manufacturing owing to its inherent advantages of process automation, fewer processing steps, being solvent free, and reduced required capital investment (H. Patil et al., 2016, MA. Repka et al., 2018). HME technique is widely used in solubility enhancement of poorly soluble drugs along with development of various novel dosage forms including abuse deterrent formulations, taste masked dosage forms and shaped delivery systems (RV. Tiwari et al., 2016). During the process of HME polymers and drugs are melted, mixed at molecular level, and pumped out through a die. The product may be in the form of powders, granules, pellets, strands, films or creams and gels depending on the application of dosage form. Process parameters such as temperature, screw speed, feed rate and pressure inside the barrel of the extruder can be controlled during the HME process and affect the quality of dosage forms (M. Maniruzzaman et al., 2012). Viscosity, thermoplasticity, deformation characteristics and softness of the materials utilized in the process plays key role in HME processability along with process parameters. Some additives like plasticizers and surfactants such as polyethylene glycols, polypropylene glycols, TPGS can aid in the HME processability at low temperatures. HME possess strengths such as customization, continuous, scalable, economic, high throughput, and solvent free nature along with weaknesses such as not suitable for thermolabile drugs, recrystallization of the products during storage and high energy requirements (M. Repka et al., 2018).

1.3 Fused deposition modeling (FDM) 3D printing

3D printing is the process of creating objects three dimensionally by depositing material in a layer by layer fashion from digital designs. The concept of 3D printing was first developed in 1980's by Charles hull for fabricating plastic devices from photopolymers (Pucci, J. U., Christophe, B. R., Sisti, J. A., & Connolly Jr, E. S. (2017). It was later used in various other fields including automotive, aerospace, robotics, and consumer goods industries for rapid prototyping purposes (Azad, M. A., Olawuni, D (2020). After FDA approval of first 3D printed pill Spritam® in 2015, the application of 3D printing has gained tremendous attraction in the pharmaceutical field (Warsi, M. H., Yusuf, M., Al Robaian, M., Khan, M., Muheem, A., & Khan, S. (2018). With advancement in pharmaceutical technologies personalization of therapies has become a prime necessity over the last decade. 3D printing is believed to be the most effective way to attain patient centric drug product development. Application of 3D printing has been an emerging field of research in pharmaceutics and drug delivery because of its ability to customize medical treatments to meet the requirements and variations of individual patients (Jamróz, W., Szafraniec, J., Kurek, M., & Jachowicz, R. (2018). With the help of 3D printing technique, it is possible to achieve precision medicine which helps in tailoring therapeutic strategies to meet the unique physiological and lifestyle needs of individual patients (Jain, V., Haider, N., & Jain, K. (2018). The advantages of 3D printing over conventional tablet manufacturing method are personalization, improved product complexity and on demand manufacturing (Norman, J., Madurawe, R. D., Moore, C. M., Khan, M. A., & Khai ruzzaman, A. (2017).

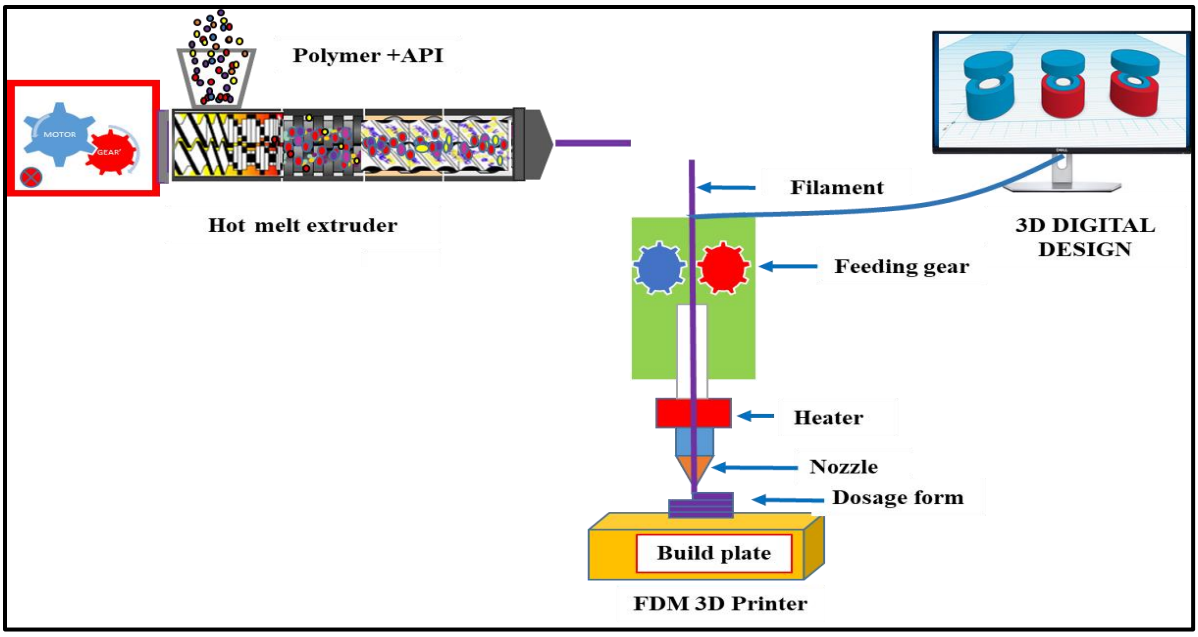

Fig.1.1 Graphical representation of hot melt extrusion coupled FDM 3D printing for fabrication of pharmaceutical dosage forms.

FDM 3D printing has capability to create customized dosage forms for personalized pharmacotherapy with its ability to produce dosage forms with complex structures, customized shapes, and sizes. Based on these advantages several research groups have developed and evaluated both traditional and novel dosage forms using FDM 3D printing for various applications. including conventional immediate release tablets and capsules, controlled and modified release dosage forms, novel floating systems for increases gastric retention, pulsatile release systems, transdermal and trans mucosal delivery systems, personalized implants, and devices.

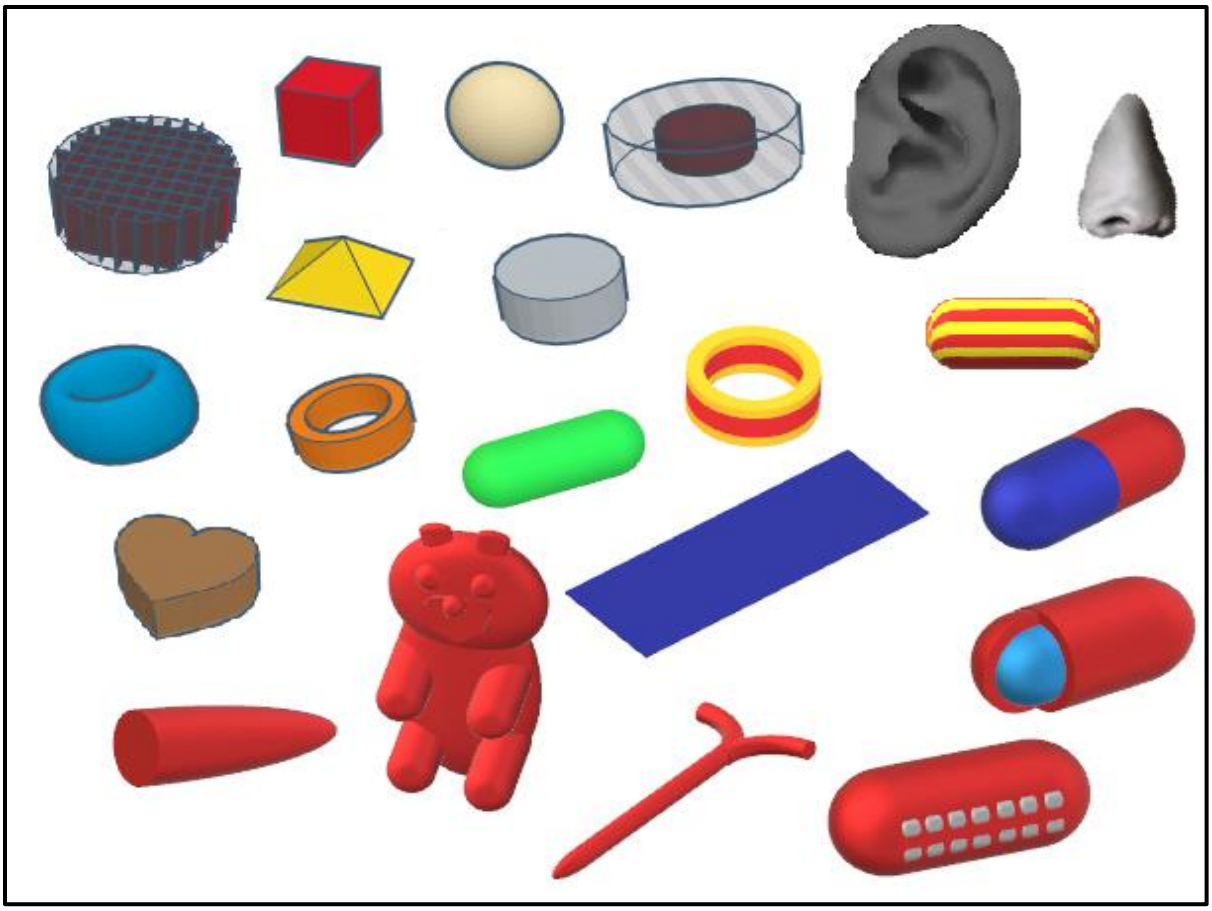

Fig. 1.2. Examples of various possible complex dosage forms those can be produced with FDM 3D printing.

1.4 Research objectives

The main objective of this work is to develop site-specific drug delivery systems to specific parts of the gastrointestinal tract using hot melt extrusion and FDM 3D printing. The aim of first project was improved treatment of chronotherapeutic disease conditions by delivering drugs to the lower part of gastrointestinal tract (colon). The scope of second project was pulsatile delivery of medication after a predetermined lag time to upper part of the gastrointestinal tract for treatment of nocturnal asthma. The objective of third research work was sustained delivery of medication to

the upper part of gastrointestinal tract to improve the treatment efficacy of narrow absorption window drugs.

1.4.1 Specific Aims

1. Chronotherapeutic Drug Delivery of Ketoprofen and Ibuprofen for Improved Treatment of Early Morning Stiffness in Arthritis Using Hot-Melt Extrusion Technology

2. Novel Gastroretentive Floating Pulsatile Drug Delivery System Produced via Hot-Melt Extrusion and Fused Deposition Modeling 3D Printing.

3. Development of sustained release Gastroretentive floating tablets using HME coupled 3D printing: A Quality by Design (QbD) approach

CHAPTER 2

. Chronotherapeutic Drug Delivery of Ketoprofen and Ibuprofen for Improved Treatment of Early Morning Stiffness in Arthritis Using Hot-Melt Extrusion Technology

2.1 Introduction

Chronotherapy deals with synchronizing drug delivery with the body's circadian rhythm to optimize therapeutic efficacy and minimize side effects (Khan et al., 2009). Diseases that follow the circadian rhythm with exacerbated symptoms at specific times of the day are targets of chronotherapeutic drug delivery systems (CTDDS). Various diseases that follow the circadian rhythm include rheumatoid arthritis, cardiovascular disorders, bronchial asthma, gastric ulcers, cancer, and some neurological disorders (Mandal et al., 2010). Among the diseases that follow circadian rhythms, arthritis is a condition characterized by exacerbated pain, joint stiffness, and swelling of the fingers in the early morning hours due to the presence of high concentrations of c-reactive protein and interleukin-6 in the plasma (Saitoh et al., 2001). Thus, the chronotherapeutic delivery of nonsteroidal anti-inflammatory drugs (NSAIDs) such as ketoprofen (KTP) and ibuprofen (IBU) could improve the quality of life of arthritis patients.

Recently, there has been a growing interest in chronotherapeutic drug delivery systems (CTDDS) with the advantage of delivering drugs at a specific time to a specific site (Roy et al., 2009). These CTDDS avoid first pass metabolism, minimize drug side effects, and mainly deliver drugs

following the body's circadian rhythm after a pre-determined lag time when the peak plasma concentration of the drug is required. Several researchers have formulated chronotherapeutic and pulsatile drug delivery systems using different strategies. Nayak et al., 2009 developed a pulsatile capsule dosage form of valsartan as a treatment model for the early morning surge in blood pressure. Jose et al. formulated colon-specific chitosan microspheres for chronotherapy of chronic stable angina. Shiohira et al., 2009 prepared a chronotherapeutic rectal aminophylline delivery system for asthma therapy. Recently, Wang et al., 2017 developed a time-adjustable pulsatile system (TAPS) for the treatment of arthritis. Although many strategies have been developed for formulating chronotherapeutic and pulsatile drug delivery systems, most of them are not suitable for scale up or for a continuous manufacturing process because their production requires several complex steps and the inclusion of solvents, is time consuming, and demands increased manufacturing costs. Therefore, we aimed to develop a CTDDS of KTP and IBU using the continuous hot-melt extrusion (HME) technique.

KTP and IBU are widely prescribed NSAIDs for the treatment of rheumatoid arthritis. Although these NSAIDs are very effective in relieving pain associated with rheumatoid arthritis, the main disadvantages are the side effects, which include gastric bleeding, dyspepsia, and peptic ulceration (Castellsague et al., 2012). Another problem that needs to be addressed regarding these drugs is their short half-life. Owing to the short half-life, the drugs need to be administered just before the onset of symptoms (i.e., in the early morning hours), which leads to patient incompliance. The chronomodulated systems offer an advantage of temporal and site-specific drug release. The reported compression coated, and coating drug core chronotherapeutic systems have complex manufacturing processes, which include multiple steps. However, hot-melt extrusion technology was reported as a continuous process with reduced downstream processing (Ye et al., 2016). Thus,

this technology was utilized to produce simple chronomodulated pellets in capsules as an alternative dosage form. To the best of our knowledge, there are no reports of chronotherapeutic drug delivery systems using HME technology for improved chronotherapy for arthritis. A drug delivery system that delivers the drug after a pre-determined lag time (approximately 6 h) and maintains the constant blood plasma concentration is required for better patient compliance and optimal therapeutic efficacy. This requirement can be fulfilled by developing a chronotherapeutic drug delivery system that delivers the drug according to the body's circadian rhythm (Pozzi et al., 1994). To achieve this, Eudragit S100 (ES100) was selected as an enteric polymer that solubilizes and releases the drug at above pH 7 i.e. in the colon. Ethyl cellulose (EC) was utilized to provide the desired lag time with slow release and maintain constant blood plasma concentrations thereafter. The main objective of the current investigation was to develop a drug delivery system to deliver NSAIDs KTP and IBU to the colon for chronotherapeutic condition asthma with a desired lag time of 6 h using an industrially feasible continuous HME process. The chemical structures of KTP (a) and IBU (b) are provided below.

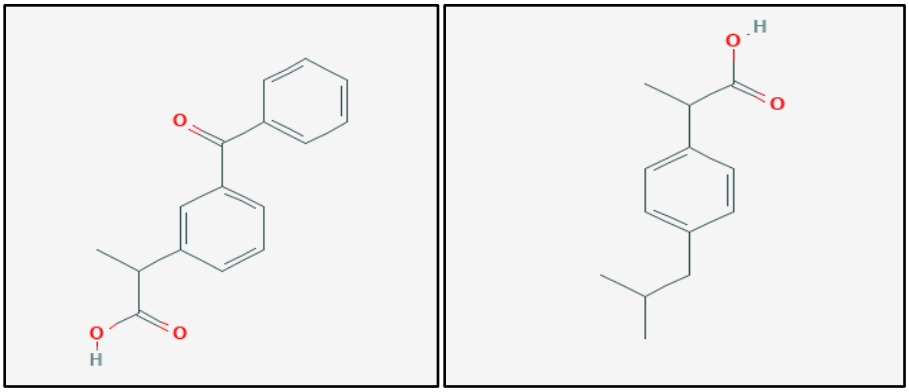

a. Chemical structure of KTP b. Chemical structure of IBU

2.2 Materials

KTP and IBU were purchased from PCCA (Houston, Texas). Eudragit S100 (ES100) was a kind gift from Evonik (Darmstadt, Germany), and ethyl cellulose (EC) was obtained from the DOW chemical company (Midland, Michigan). All other reagents used were purchased from Fisher Scientific and were of analytical grade.

2.3 Methods

2.3.1 HME Processing

The polymers and drugs were sifted using a sieve (USP #30 screen size) and dried in an oven at 40°C to remove any residual moisture present. The materials were blended using a twin shell V-blender (GlobePharma, Maxiblend®) at 25 rpm for 15 min. Preliminary experiments were performed initially using a 6-mm counter-rotating mini extruder (Haake Minilab, Thermo Electron, Germany), and thereafter optimized formulations were finally extruded using the pilot scale 16-mm co-rotating twin screw extruder with a standard screw configuration as shown in Fig. 1 (16 mm, Prism Euro Lab, Thermo Fisher Scientific). The composition of different formulations, processing parameters, and percent drug released after lag time (6 h) using the 6-mm extruder is listed in Table I. Formulation compositions and processing parameters of experiments on the 16-mm extruder are listed in Table II. Initial extrudates obtained during the extrusion process were discarded until the extruder had attained a steady state, and then extrudates collected were cooled at ambient temperature and pelletized simultaneously using a pelletizer into pellets of 1, 2, and 3 mm in size. The extrudates were also milled using a comminuting mill (Fitzpatrick, model L1A) and sieved using a USP mesh screen (#25). The pellets were stored in poly bags in a desiccator until further evaluation.

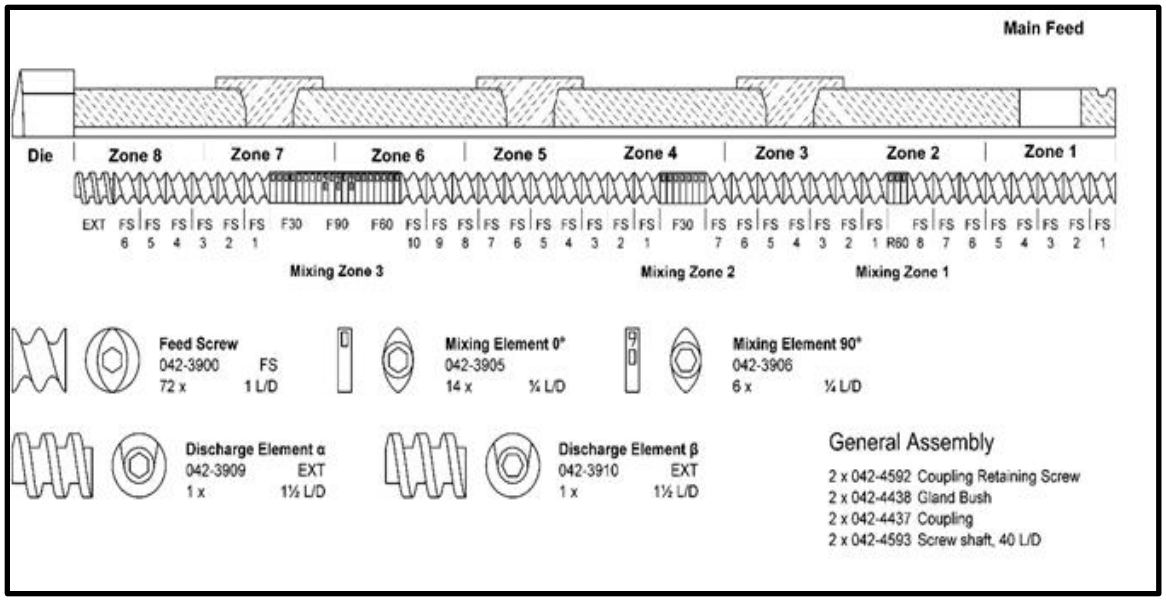

Fig. 2.1. Schematic diagram of standard twin screw configuration employed in the study.

2.3.2 Solid-State Characterization

2.3.2.1Thermogravimetric Analysis

The thermal stability of all materials used in formulations was determined using a PerkinElmer Pyris 1 thermogravimetric analyzer (TGA) equipped with Pyris manager software (PerkinElmer Life and Analytical Sciences, 719 Bridgeport Ave., CT, USA). Each sample weighing 3–5 mg was taken and heated at a heating rate of 10°C/min from 20 to 250°C.

2.3.2.2 Differential Scanning Calorimetry (DSC)

A differential scanning calorimeter (DSC 25 Series, TA instruments) was used to assess the thermal characteristics and compatibility of polymers with KTP and IBU. Samples (pure KTP, pure IBU, ES100, EC, physical mixtures, and extrudates) weighing 5–10 mg were hermetically sealed in an aluminum pan and heated at a rate of 10°C/min from 25 to 150°C. Ultra-pure nitrogen was used as the purge gas at a flow rate of 50 mL/min.

2.3.2.3 Powder X-ray Diffraction (PXRD)

The solid state of KTP, IBU, ES100, EC extrudates, and the respective physical mixtures was investigated using a powder X-ray diffraction apparatus (Bruker AXS, Madison, MI) using CuKα radiation at a 40-kV generator voltage and 40 mA current. The diffraction angles were 5–40° (2θ), and the scanning rate was set at 2°/min.

2.3.2.4 FTIR Spectroscopy

The molecular interactions of KTP and IBU with polymers, before and after HME processing, were analyzed by FTIR spectroscopy. The studies were performed on an Agilent Technologies Cary 660 (Santa Clara, CA) instrument. The bench was equipped with an ATR (Pike Technologies MIRacle ATR, Madison, WI) that was fitted with a single bounce diamond coated ZnSe internal reflection element. The scanning range was 400–4000 $cm^{-1.}$

2.3.3 *In vitro* Dissolution Study

Three-stage dissolution testing was performed according to the USP XXIII paddle method using an SR8-plus Hanson dissolution apparatus. Firstly, dissolution was conducted in 750 mL of 0.1 N HCl for 2 h. In the second stage, after 2 h, the pH was increased to 6.8 by addition of 250 mL of 0.2 M sodium triphosphate buffer, and dissolution was carried out for 4 h. In the third stage, the pH of the dissolution medium was adjusted to pH 7.4 with 0.1 M sodium hydroxide, and dissolution was conducted up to 24 h. Paddle rotation was set at 50 rpm, and the temperature of the dissolution medium was maintained at 37 ± 0.5°C. Samples (3 mL) were collected at pre-determined intervals, and KTP and IBU contents were quantified using a HPLC system.

2.3.4 HPLC analysis of NSAIDs

2.3.4.1 Ketoprofen

The content of KTP present in the in vitro samples was quantified using a HPLC system (Waters Corp, Milford, MA, USA). For KTP (method stated in USP-NF was used), a Phenomenex Luna® C18 reverse phase column (5 µm, 100 Å, 250 × 4.6 mm) was used as the stationary phase. The mobile phase consisted of water, acetonitrile, and glacial acetic acid (90:110:1). The flow rate was maintained at 1.2 mL/min, and the UV-detector was set at 256 nm (Waters 2489 UV/detector). Twenty microliters were injected from each sample, and the data was analyzed using Empower 2 software. A six-point calibration curve was plotted and found to be linear in the concentration range of 2 µg/mL to 100 µg/mL with a correlation coefficient (R2) of 0.999. The limit of detection and limit of quantification values for the method were found to be 0.2µg/mL and 0.7 µg/mL, respectively.

2.3.4.2 Ibuprofen

The IBU content was analyzed using a Phenomenex Luna® C18 reverse phase column (5 µm, 100 Å, 250 ×4.6 mm) stationary phase, and the mobile phase consisted of water, acetonitrile, and chloro acetic acid (40:60:0.01) (USP-NF). The flow rate was 2 mL/min, sample volume was 10 µL, and the UV-detector was set at 221 nm (Waters 2489 UV/detector). Empower 2 software was used to analyze the data. A calibration curve plotted was found to be linear in the concentration range of 1 µg /mL to 100 µg /mL with a correlation coefficient (R2) of 0.999. The limit of detection and limit of quantification values for the method were found to be 0.3µg/mL and 1µg/mL, respectively.

2.3.5 Scanning Electron Microscopy (SEM)

The surface morphology of pellets before dissolution and during dissolution of both KTP and IBU was assessed using a JSM-5600 scanning electron microscope (JEOL USA, Inc., Waterford, VA, US). The pellets at 0 h and at different time points in the dissolution media (2 h in 0.1 N HCL; 6 h in pH 6.8 phosphate buffer; and 7, 10, and 12 h in pH 7.4 phosphate buffer) were collected, placed in a sieve, and air dried for 24 h to remove any water content present. These dried pellets were sputter coated with gold under an argon atmosphere using a Hummer 6.2 Sputter Coater (Ladd Research Industries, Williston, VT, USA), and surface morphology was observed using a JSM-5600 scanning electron microscope at an accelerating voltage of 5 kV.

2.3.6 Stability Studies

Formulations (KTP1-3MM, IBU1-3MM) were stored at accelerated stability conditions (i.e., at 40°C/75% RH). The formulations were evaluated physically and tested for drug content and in vitro dissolution release profiles. Physical appearance was observed and noted. The similarity factor was calculated using the following equation.

$$f2 = 50\log\left\{\left[1 + \frac{1}{n}\sum_{t=1}^{n} Rt - Tt\right]^{-0.5}\right\}x100$$

Rt and Tt are the cumulative percentage dissolved at each of the selected n time points of the reference and test product, respectively. The value of the similarity factor ranges from 1 to 100, and if the values approach 100, the similarity between the test and reference product increases. The similarity factor should be above 50 to consider the test and reference products similar.

2.4 Results and discussion

2.4.1 HME Processing

Preliminary experiments performed using a 6-mm extruder (Haake Minilab, Thermo Electron, Germany) to assess the feasibility of the processing parameters (temperature, feed rate,rpm) provided the data to optimize the conditions without any thermal degradation of the materials used. ES100, KTP, and IBU were selected as the enteric polymer and drugs, respectively. KTP and IBU are frequently indicated in treatment of arthritis (a condition target of the chronotherapeutic drug delivery system). ES100 has a high glass transition (Tg) temperature of 172°C, as reported previously (28). KTP and IBU exhibited melting points at 94 and 78°C, respectively (Determined by DSC, TA 25SERIES). Both KTP and ES100 undergo thermal degradation above 180°C and IBU above 150°C (29). Usually, extrusion of polymers is carried out above the glass transition temperature for the polymer to have sufficient mobility inside the extruder and to maintain the torque value below the maximum level where the motor cannot function. Plasticizers, which increase molecular chain mobility and reduce frictional forces between polymer chains, are used to reduce the glass transition temperature, facilitating smooth HME processing at low temperatures (30). The two model drugs employed in this study, KTP and IBU, can act as plasticizers, so no plasticizers were used in the present study.

In preliminary experiments carried out on a 6-mm extruder, ES100 and KTP were extruded at 30, 40, and 50% drug load. Extrudate strands of 30 and 40% drug load formed a coalesced matrix and were transparent, whereas with 50% drug loading, extrudates were not transparent and the formulation flowed out as a liquid because of the high KTP content. When the processing temperature was further decreased to obtain coalesced extrudate strands, ES100 was observed as distinct particles and phase separation occurred, which can be due to non-melting of ES100. In

vitro dissolution testing was carried out for 30 and 40% drug loading of KTP to understand the release pattern (results not shown), and the results showed above 50% within 6 h with no desired lag time, which was not suitable for the desired chronotherapeutic drug delivery system. Similarly, IBU extrudates with ES100 released the maximum drug within 6 h.

In the next stage, EC, a hydrophobic polymer, was added to the formulation (2.5, 5, and 10%) to retard the initial drug release beyond 6 h. The dissolution profile revealed that EC was able to retard the drug with a minimum amount of drug released in the first 6 h (less than 20%). Based on these preliminary experiments and the results for both KTP and IBU, further trials were carried out on a 16-mm extruder with optimized formulations, as one of the objectives of the current investigation was to develop an industrially feasible chronotherapeutic drug delivery system.

KTP with 40% drug loaded with EC (2.5% and 5%) and ES 100 were extruded at a temperature of 120°C, screw speed of 100 rpm, and feed rate of 5 g/min. The extrudates obtained were coalesced and transparent, as shown (Fig. 2A). Similarly, the extrusion was carried out with IBU at 40% drug loading with EC (2.5% and 5%) and ES100 at 100°C, 100 rpm screw speed, and 5 g/min feed rate. The images of the extrudates are shown in Fig. 2B.

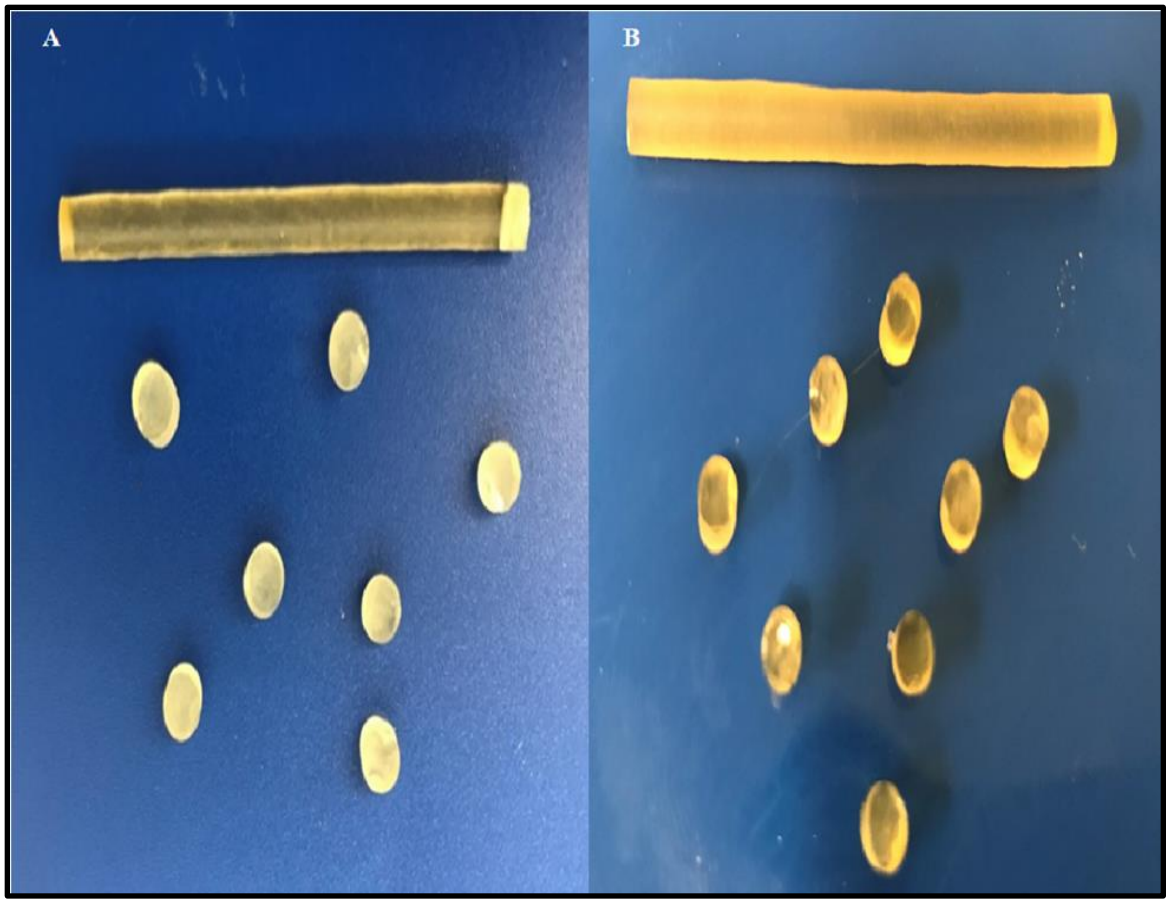

Fig. 2.2 Images of extruded strands and pellets (3 mm) of KTP (a) and IBU (b)

2.4.2 Solid state characterization

The TGA results showed that APIs and polymers were stable at the processing temperatures employed during HME. The DSC thermograms of KTP, IBU, ES100, EC, physical mixtures of drug and polymers, and extrudates are shown in Fig. 3. The DSC thermograms of pure KTP and IBU showed sharp endotherms at 78°C and 94°C, corresponding to their melting points. The intensities of these peaks were reduced in the physical mixtures (PM). In both the KTP and IBU extrudates, these characteristic endotherms disappeared, indicating the amorphous nature of APIs in the extrudates and the complete miscibility of drugs and polymers. This was further confirmed by the PXRD studies. In PXRD (Fig. 4), KTP had major characteristic peaks at 6.3,

13.1, 17.3, and 22.9o, and IBU showed peaks at 6, 16.5, 19.5, and 22o. The intensities of the peaks were reduced in physical mixtures, and complete absence of peaks was observed in extrudates, in correlation with DSC thermograms, substantiating the amorphous nature of KTP and IBU in the formulations. This conversion of crystalline drugs into an amorphous nature may be attributed to the molecular mixing of components in the molten form during melt extrusion.

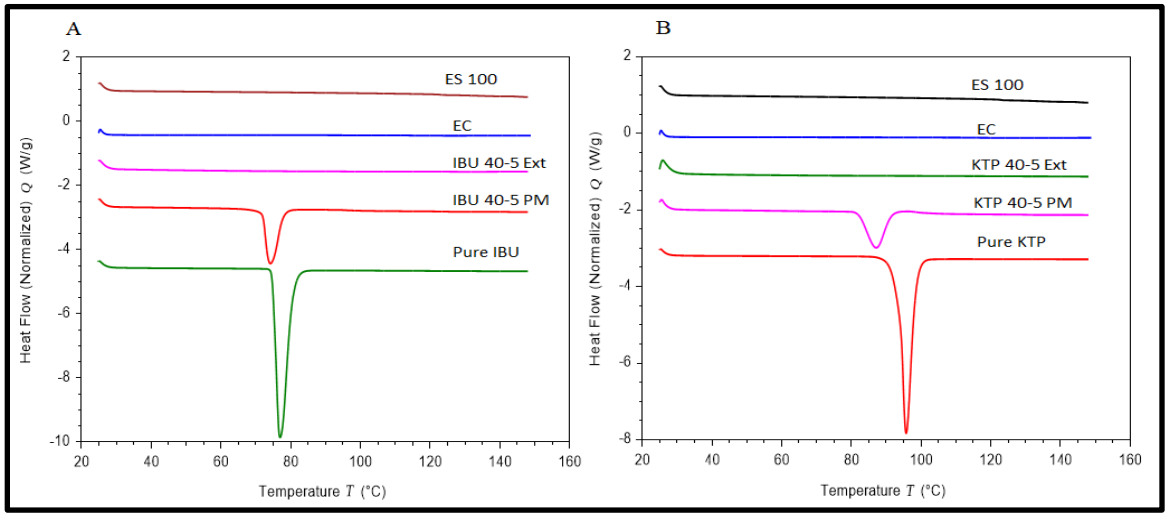

Fig. 2.3 DSC thermograms of (a) ES 100, EC, IBU 40-5Ext, IBU 40-5PM, Pure IBU (b) ES 100, EC, KTP 40-5Ext, KTP 40-5PM, Pure KTP.

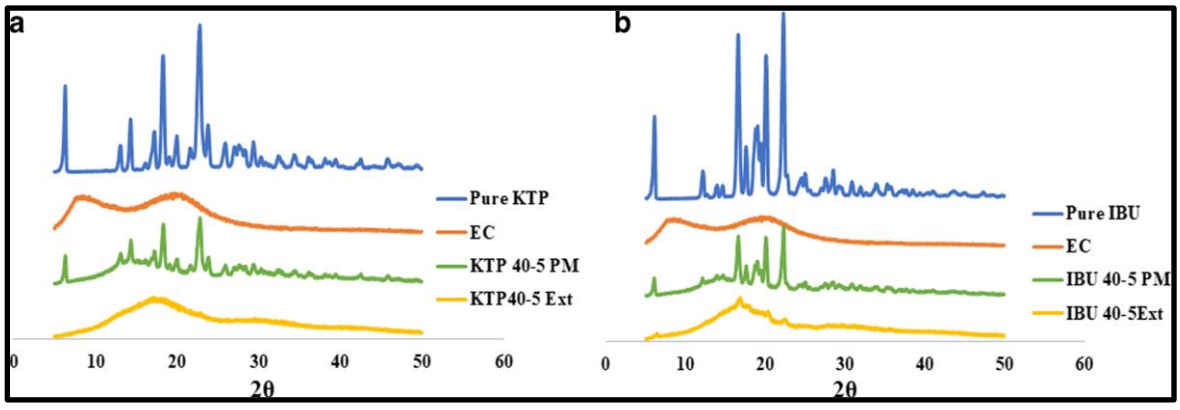

Fig. 2.4 PXRD of (a) EC, KTP 40-5 Ext, KTP 40-5PM, Pure KTP (b) EC, IBU 40-5Ext, IBU 40-5PM, Pure IBU.

2.4.3 Fourier transform infrared (FTIR) spectroscopy.

FTIR spectra of pure KTP, IBU, ES100, EC, physical mixtures, and formulations are shown in Fig. 5. FTIR spectra showed major characteristic peaks of KTP at wavenumbers 1693, 1653, 1282, 714, and 702 cm^{-1}. These major characteristic peaks were observed in the physical mixture and extrudate formulations, suggesting the absence of intermolecular interactions between the drug and other polymers utilized in the formulations. Similarly, IBU had characteristic peaks at 2952, 1709, and 779 cm-1 both in the physical mixture and formulation compared with pure IBU, indicating absence of interactions. These results suggest the suitability of the materials in the of formulation of chronomodulated systems of KTP and IBU for treating early morning symptoms rheumatoid arthritis.

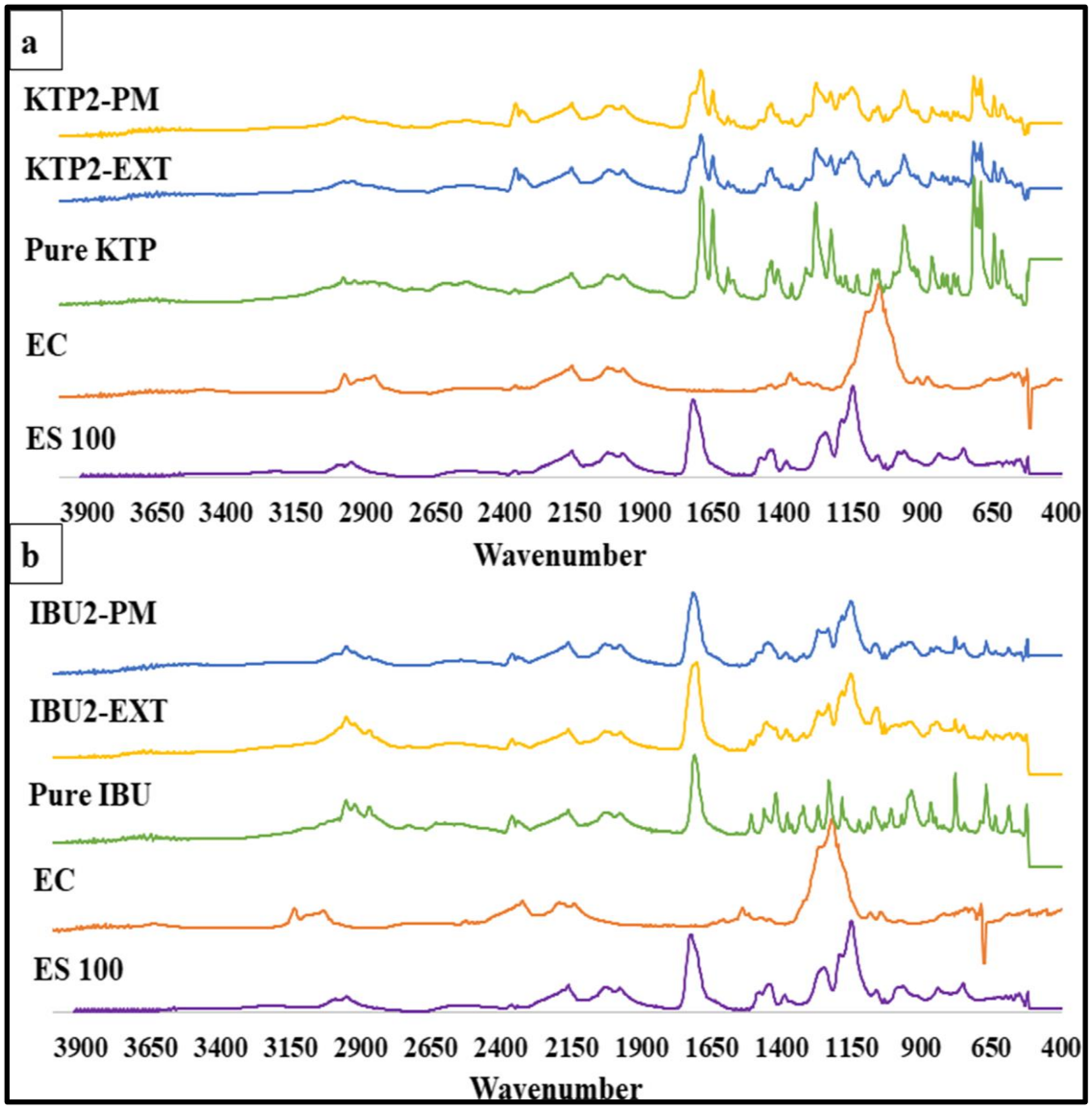

Fig. 2.5. FTIR spectra of KTP, IBU, polymers, physical mixtures (PM), and extrudate (EXT) formulations

2.4.4 *In vitro* dissolution study

The *in vitro* drug release studies performed in different pH conditions to assess the suitable chronotherapeutic formulation showed the desired lag time. In this investigation, formulations with < 20% drug release in 6 h (lag time) were considered to meet the requirements of the optimized chronotherapeutic drug delivery system to relieve the symptoms of rheumatoid arthritis conditions in the early morning. The *in vitro* dissolution profiles of KTP and IBU formulations are shown in

Fig. 6 and Fig. 7, respectively. The dissolution rate of both the drugs was influenced by the concentration of EC and the size of the extrudate pellets.

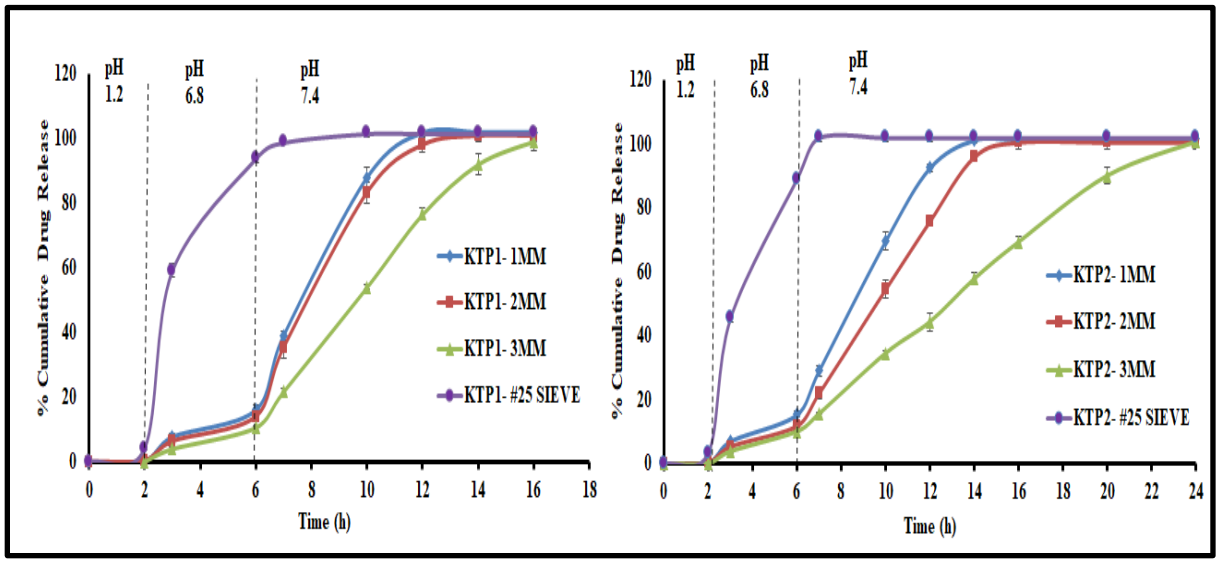

Fig. 2.6. In vitro drug release profile of the KTP formulation containing 2.5% EC and 5% EC with different pellet sizes

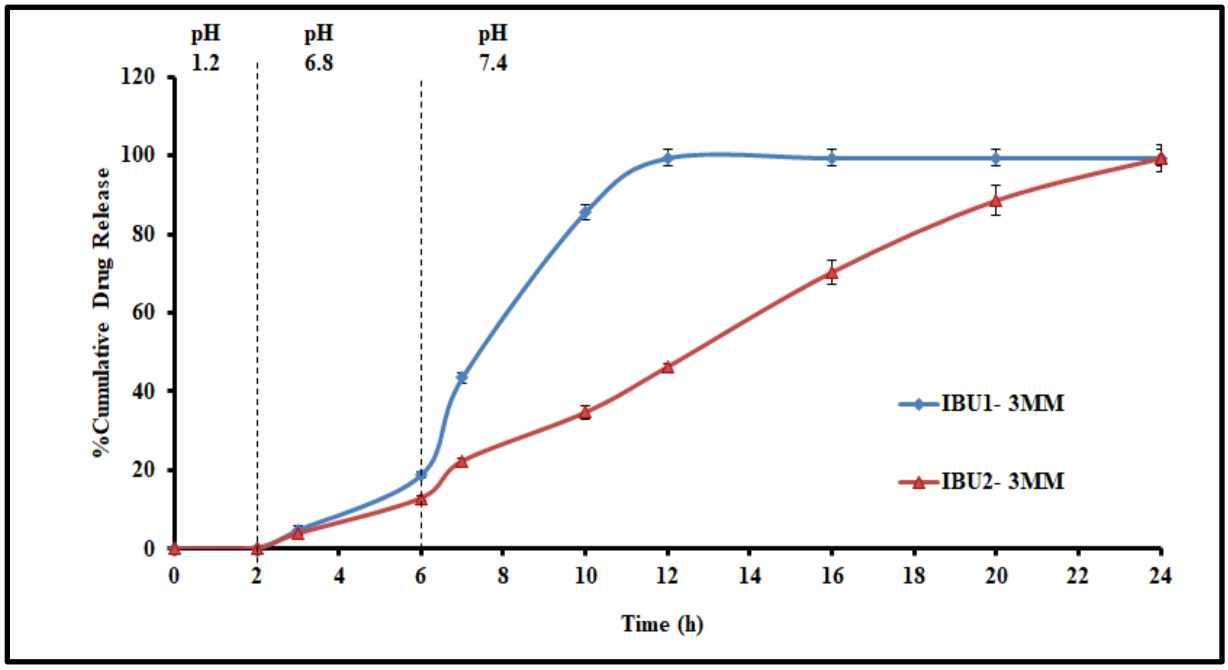

Fig. 2.7. In vitro drug release profile of the IBU formulation containing 2.5% EC and 5% EC with 3 mm pellet size

2.4.4.1 Effect of pellet size

The dissolution profile of the drug from different formulations is dependent on the pellet size of the extrudates. In pH 1.2 media after 2 h, less than 0.5% of the drug was released from the KTP pellets compared to approximately 3.4–4.2% drug release observed in the pulverized formulations (KTP1- #25SIEVE and KTP2- #25SIEVE). At the end of 6 h in pH 6.8 buffer, the drug release from different sized pellets with 2.5% EC was in the range of 10.6–15.0%. Similar results were observed with the formulation composed of 5% EC (10.1–14.6%). The formulations, with 2.5% or 5% EC in pH 7.4 media, showed a complete drug release and a sustained drug release from the 3 mm size pellets compared to that from the smaller sized pellets (1 and 2 mm). These results ascertain that the drug release is influenced by the pellet size, as discussed in the earlier literature reports (31, 32). Moreover, a complete drug release (90% and 94%) from powdered formulations was observed at pH 6.8, and this was significantly different ($p < 0.05$) than that observed in the pellets. This is attributed to the increased surface area due to the smaller particle size of the powdered formulation. Sustained drug release from the larger pellet size could be attributed to either the lower surface area of the larger pellets compared to the smaller pellets or increased average distance for diffusion of the active ingredient from the pellet (33).

2.4.4.2 Effect of ethyl cellulose

In addition to pellet size, a remarkable impact of EC composition on drug release behavior was observed. As the composition of the EC increased, the pellets showed more sustained drug release profiles. A 100% drug release from 1, 2, and 3 mm pellets with 2.5% EC was noticed at 12, 14, and 16 h, respectively, while the drug release was sustained for 14, 16, and 22 h, respectively, from pellets containing 5% EC. This marked difference in dissolution profiles of pellets with 2.5% and 5% EC supports the fact that EC maintains the matrix integrity for a longer

time at a high concentration. Further, 90% and 94% drug release from the powdered formulations in 6 h could be correlated with the weak matrix integrity due to loss of EC during the pulverization. Figure 4 delineates the drug release profile of IBU. The dissolution profile data shows that results were in correlation with KTP, with a slight variation in the amount of drug released at lag time. Since 18% drug release was observed from 3 mm pellets (2.5% EC) at lag time (6 h), no other sized pellets of IBU were fabricated and evaluated (as formulations with <15% drug release at lag time were set to be suitable for chronotherapeutic systems). As observed with the KTP in vitro results, the 3 mm pellets of IBU with 2.5% EC showed a 12 h drug release profile while the pellets with 5% EC sustained drug release for 24 h.

From the above in vitro dissolution results for KTP and IBU, formulations of KTP1-1MM and IBU1-1MM showed 100% drug release in 12 h, which could relieve the early morning symptoms of arthritis with the required therapeutic concentrations. The 3 mm KTP and 3 mm IBU showed sustained release. The correlation coefficient values of all the formulations of KTP or IBU showed a good correlation to the zero-order equation (r^2= 0.9712–0.9998) and high linearity when compared to other models, suggesting that drug release followed the zero order. From the above results, it can be inferred that a chronotherapeutic drug delivery system can be developed using HME technology with desired drug release characteristics.

2.4.5 Scanning electron microscopy (SEM)

SEM images of KTP pellets (Fig. 8a) obtained from the dissolution vessel, at different time points, elucidated the surface morphological changes that occurred during the dissolution process, further confirming the drug release mechanism from the matrix. The intact surface of the 3 mm KTP pellet at pH 1.2 at 2 h (B) ensured low or no drug release. The appearance of small cracks on the surface of the pellets obtained from pH 6.8 media supported the minimum drug release at 6 h

(C). The intensity of cracks and the dissolution rate increased as the pH of the dissolution changed to 7.4 (D). The increased intensity of the cracks may be caused by the dissolving nature of the Eudragit at above pH 7. The reduction in pellet size was observed from images taken at 10 and 12 h (E, F). In SEM images of IBU (Fig. 8b), the film formation by EC on the surface of the pellets was not clearly observed, and the intensity of cracks was less when compared to KTP. A hole formation was observed (F) in pellets along with a size reduction. This may be caused by a variation in solubility of IBU in the dissolution media compared to KTP.

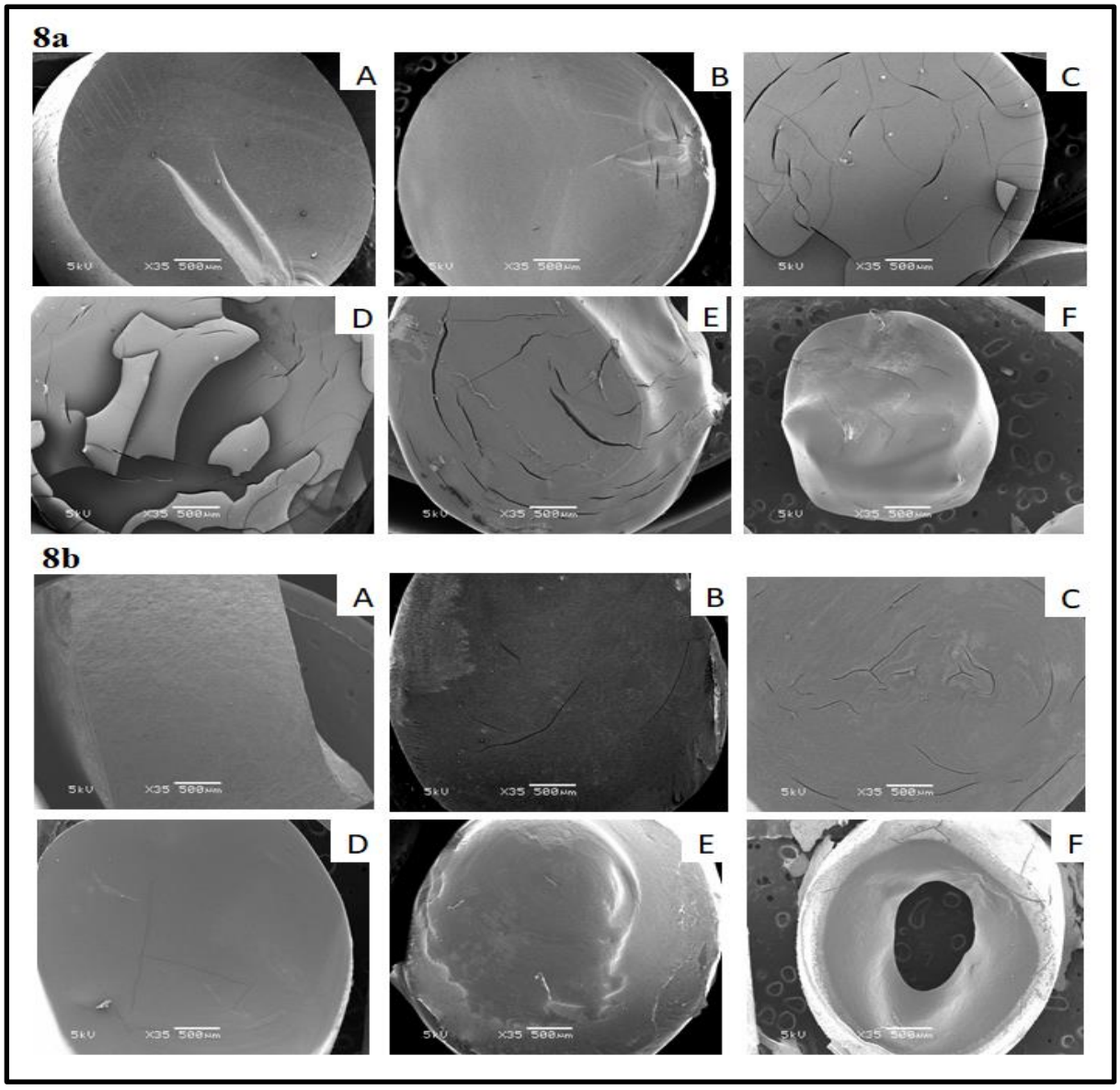

Fig. 2.8. SEM images of (i) KTP and (ii) IBU pellets taken from dissolution media at different time points (a) 0 h, (b) 2 h, (c) 6 h, (d) 7 h, (e) 10 h, and (f) 12 h

2.4.6 Stability study

The stability of the formulations at accelerated stability conditions (45°C and 75% RH) for both KTP and IBU showed stability over 4 months. The stability samples were characterized for drug release properties and drug content. The *in vitro* drug release studies performed after the 4th month showed similar release profiles compared to those of the initial samples. The similarity

factor (f2) value was above 70, confirming the similar release profile and stability. Drug content (n=3) was found to be in the range of 96–103%. Further, the extrudates did not show any change in physical appearance after 3 months of accelerated stability study. Dissolution profiles of formulations KTP1-3MM and IBU1-3MM initially and at 4 months are shown in Fig. 9.

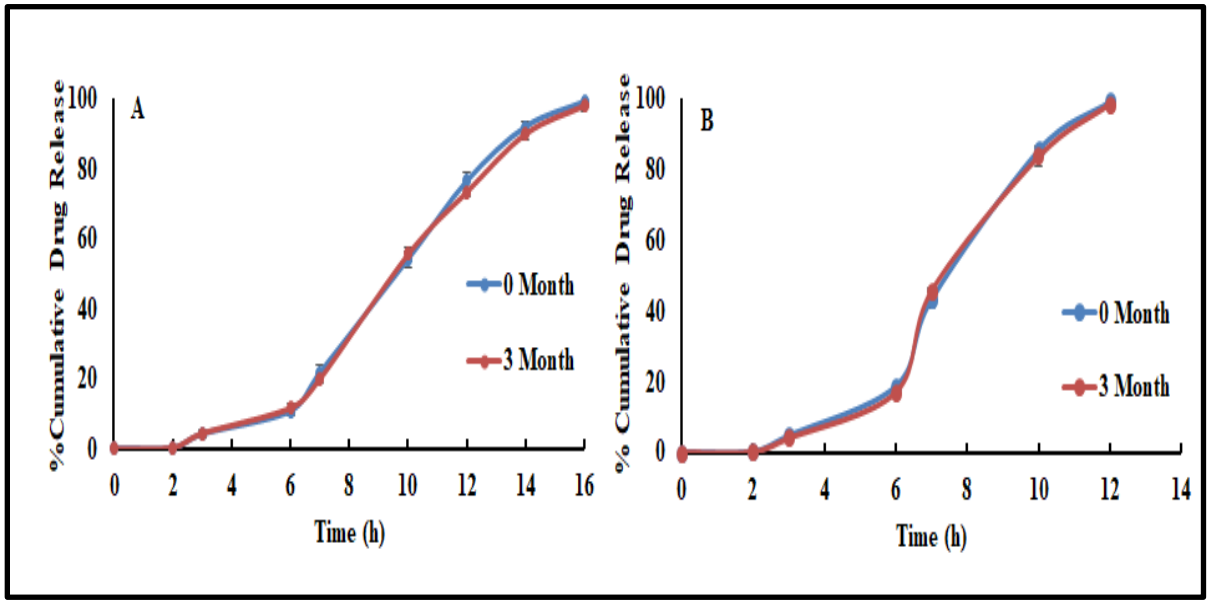

Fig. 2.9. In vitro release profiles of IBU1-3MM (a) and KTP1-3MM (b) initially and after 4 months of accelerated stability study.

2.4.7 Conclusion

A chronotherapeutic drug delivery system for KTP and IBU was successfully developed for the treatment of arthritis conditions in the early morning hours. The drug release studies conducted in different media showed the desired lag time and release characteristics. The concentration of ethyl cellulose and size of extrudate pellets had significant effects on *in vitro* drug release profiles. Ethyl cellulose at low concentrations of 2.5% and 5% can act as a potent release retarding agent in the HME techniques. Furthermore, the developed formulations need to be assessed *in vivo*. In conclusion, HME is a novel, viable technique suitable for developing a

chronotherapeutic drug delivery system with many advantages compared to those of other traditional techniques.

CHAPTER 3

Novel Gastroretentive Floating Pulsatile Drug Delivery System Produced via Hot-Melt Extrusion and Fused Deposition Modeling 3D Printing.

3.1 Introduction

Maintaining a constant plasma drug concentration is not beneficial in all disease conditions. Some diseases may require pulse delivery of drugs to avoid unwanted adverse effects and drug exposure. Certain diseases, such as bronchial asthma, angina pectoris, ulcers, and rheumatoid arthritis, are regulated by the circadian rhythm of the body and require drug administration at specific times of a day, particularly in the early morning hours. Such diseases require pulsatile drug delivery after a lag time to improve patient compliance and drug adherence. Pulsatile drug delivery systems (PDDS) provide a timely pharmacological effect to the patient preventing unwanted sustained drug exposure. PDDS will not interrupt patients normal sleep patterns following an evening dose of medication. Moreover, pulsatile systems can prevent detrimental drug-drug interactions without changing the administration schedule of patients taking multiple medications at the same time and can enhance patient compliance (Thitinan et al., 2012, Jain et al., 2011, Sunil et al., 2011]. To address these issues, a drug delivery system that delivers a pulsatile release of drugs after a pre-determined lag time is necessary. Thus, drugs administered at bedtime would be released in the early morning hours and be available to alleviate the symptoms and improve the quality of life of the patients.

Various biological factors influence the transit time of drugs in the upper gastrointestinal tract and possess a challenge to the drugs that are locally active in the stomach, unstable at a high pH, or poorly soluble in the lower parts of the gastrointestinal tract (Maroni et al., 2010). A strategy to increase the residence time of the drugs to overcome the above-mentioned drawbacks is necessary for optimal therapeutic outcomes. Numerous strategies have been used to increase the residence time of the dosage forms in the stomach, including mucoadhesive systems, high-density systems that sink to the bottom of the stomach, swelling systems, and floating systems (Almutairy et al., 2016). Among these strategies, floating systems are considered superior as they do not interfere with the physiological activity of the gastrointestinal tract. Floating systems are further subdivided into effervescent and non-effervescent floating systems. The effervescent systems use gas-forming agents, whereas the non-effervescent systems are formulated with gel-forming polymers or hollow microspheres.

Hot-melt extrusion (HME) is a well-known technique used in the plastic, rubber, and food industries. Since the last three decades, its use in drug delivery and research has tremendously increased owing to the advantages associated with this technology, such as high efficiency, solvent-free, innovative applications, and continuous manufacturing. Although HME is the most widely used in the preparation of amorphous solid dispersions, it is also used in the development of many innovative applications, such as taste masking, abuse-deterrent formulations, chronotherapeutic systems, topical formulations, semi-solid dosage forms, and co-amorphous systems. Recently, the interest of researchers has shifted to additive manufacturing of pharmaceutical dosage forms where HME is combined with three-dimensional (3D) printing.

Three-dimensional printing is a process in which digitally controlled 3D objects are produced by the deposition of materials in a layer by layer manner. Previously it was widely used in automobile, robotics, aerospace, and other industries for rapid prototyping purposes. Because of the widespread availability of commercial 3D printers and the recent FDA approval of the first 3D printed dosage form (Spritam), its use in pharmaceutical research has greatly increased (Trenfield et al., 2018]. The main reason for the increased attention of researchers on 3D printing is because of its potential to create complex, customized, and personalized-on-demand dosage forms. Recently, fused deposition modeling (FDM) 3D printing has been used in the preparation of various novel drug delivery systems, such as personalized vaginal progesterone rings , channeled tablets for superior disintegration and dissolution, personalized oral delivery devices, and topical nose-shaped device for the treatment of acne (Goyanes et al., 2018).

In this study, HME technology-paired FDM 3D printing and conventional direct compression methods were utilized to produce novel core-shell floating pulsatile tablets with a predetermined lag time. Asthma is a chronic inflammatory condition of airways and symptoms of this condition include shortness of breath, chest tightness and coughing which are worsened at early morning hours due to regulation of circadian rhythm. So, theophylline, which is widely used for the symptomatic treatment of chronic asthma, was chosen as a model drug. However, the in vivo performance of the developed drug delivery system will be investigated in our future studies. The significance of the developed drug delivery system is to achieve both floating characteristics and pulsatile release after the desired lag time to improve therapy and quality of life of patients with asthma.

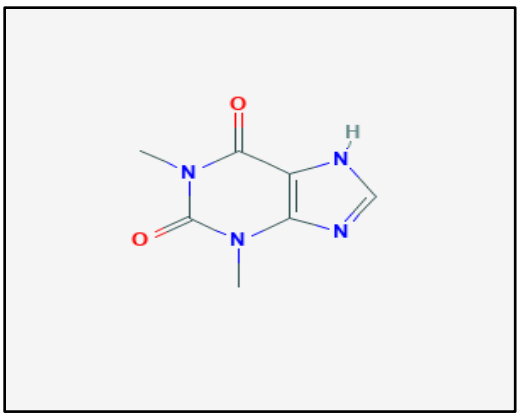

Chemical structure of Theophylline

3.2 Materials

Theophylline anhydrous (≥ 99% pure) was purchased from Sigma-Aldrich (St. Louis, MO, USA). Hydroxypropyl cellulose (HPC, Klucel LF) and ethyl cellulose (EC, Aqualon EC N14) were donated by Ashland Inc. (Covington, KY, USA). Croscarmellose sodium (Ac-Di-Sol®) and microcrystalline cellulose (Avicel PH® 102) were provided by FMC Biopolymer (Newark, DE, USA). Magnesium stearate was purchased from Alfa Aesar (Tewksbury, MA, USA). All other reagents and chemicals used were of analytical grade.

3.3 Methods

3.3.1 Thermogravimetric analysis

A thermogravimetric analyzer (TGA 1-Pyris, PerkinElmer, Inc., Waltham, MA, USA) was used to determine the thermal degradation of the polymers at the temperature employed in HME and 3D printing techniques. The samples were loaded in aluminum pans and heated from 50 °C to 500 °C at a rate of 20 °C/min. Ultra-purified nitrogen was used as a purge gas at a flow rate of 25 mL/min. The data were collected and analyzed using the PerkinElmer Pyris™ software, and the percent mass loss was calculated.

3.3.2 Preparation of the filaments using HME.

An 11 mm twin-screw co-rotating hot melt extruder (Process 11 Thermo Fisher Scientific, DE, USA) was used to prepare the filaments required for 3D printing of the floating pulsatile tablets. The standard screw configuration with 3 mixing zones was employed at 50 rpm screw speed in this study. After the filaments exited from the extruder die, a conveyor belt was used to straighten and collect the filaments for easy processing into the 3D printer. Two formulations, HPC alone (100% w/w) or in combination with EC (99.5 w/w% HPC, 0.5% w/w EC)) were mixed in a V-shell blender (Maxiblend®, Globe Pharma, New Brunswick, NJ, USA) for 15 min and used for fabrication of the filaments. A temperature of 165 °C was set in all the eight heating zones and torque inside the barrel was observed between 4−5 Nm during the extrusion process. After the extrusion process, the filaments obtained were stored in a desiccator to avoid any moisture pickup before using for 3D printing of the tablets.

3.3.3 Mechanical characteristics of hot-melt extruded filaments

The mechanical properties of the extruded filaments (flexibility or ductility and brittleness) are the critical parameters that are used to determine the suitability of the filaments for FDM 3D printing (Repka-Zhang test). Texture analyzer (TA-XT2i analyzer and Texture Technologies, Hamilton, MA, USA) were used to evaluate the mechanical properties of the filaments. The filaments were cut into a length of 5 mm and placed on the bottom flat surface of the texture analyzer. The top blade part of the texture analyzer was moved down until it penetrated the filament (0.6 mm) to create a 35% deformation in the shape of the filament. Testing for each single filament formulation was repeated 6 times. The force required to deform the filament was measured and analyzed using Exponent software version 6.1.5.0 (Stable Micro Systems, Godalming, UK). The parameters for the test were as follows: pre-test speed, 10 mm/sec; test

speed, 5 mm/sec; and post-test speed 10 mm/sec (Figure 1). The force applied by the feeding gears of the FDM 3D printer on the filament during the feeding process could be co-related with the force applied by the texture analyzer. This will give a preliminary data for the assessment of the 3D printability of extruded filaments. Polylactic acid (PLA) filaments were used as the reference standard for these measurements. The PLA has molecular weight of 66000 g/mol, glass transition temperature (T_g) of 55 °C. The PLA filaments has a diameter of 1.75 mm and tensile modulus of 3600 MPa and yield strength of 60 MPa.

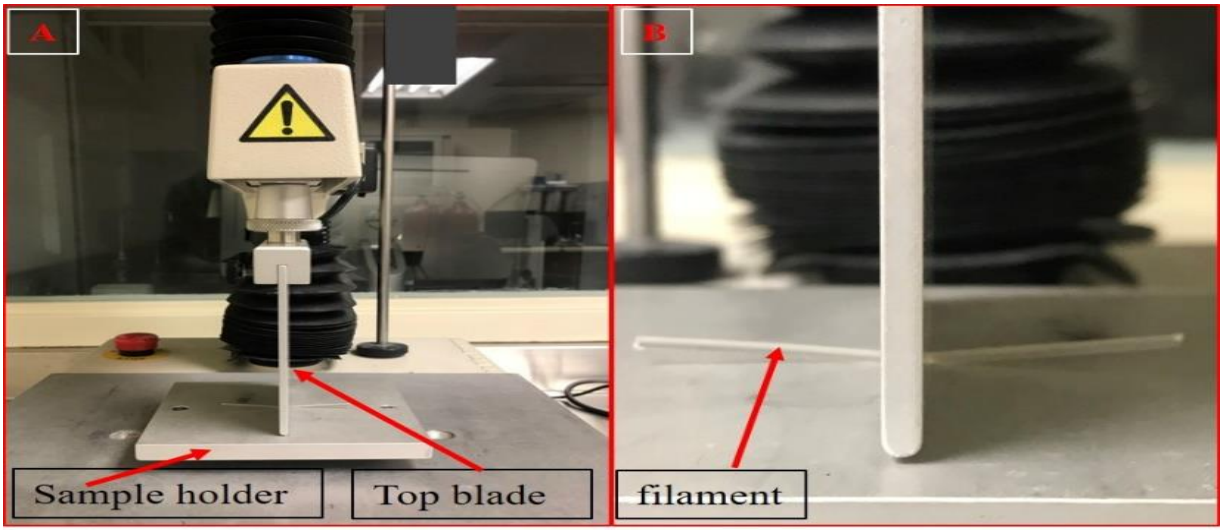

Fig. 3.1. Texture analyzer set up (A) stiffness test of the extruded filaments (B).

3.3.4 Preparation of the core tablets by direct compression

Theophylline (57% w/w), croscarmellose sodium (8% w/w), microcrystalline cellulose (34% w/w) and magnesium stearate (1% w/w) were sifted using a #30 sieve and blended using V-shell blender (Maxiblend®, Globe Pharma, New Brunswick, NJ, USA) for 10 min. The blended physical mixture (175 mg) equivalent to 100 mg of theophylline was compressed into tablets using 8 mm round flat punches by a single punch press (MCTMI, GlobePharma Inc., New Brunswick, NJ, USA).

3.3.5 3D printing of pulsatile floating tablets

Initially, the hollow tablets were designed using Autodesk® Tinkercad™ free online software and saved into 3D printer readable stl. format files. The stl. files were then imported into Ultimaker Cura software (Cura version 4.0, Ultimaker, Geldermalsen, Netherlands). Hot-melt extruded filaments were loaded into an FDM 3D printer (Prusa i3 3D desktop printer, Prusa Research, Prague, Czech Republic) having an E3D v6 Hot End and a 0.4 mm nozzle and the floating tablets were printed. All the tablets were designed to have the same dimensions (14.5 mm diameter and 7 mm height) but with different shell thicknesses, wall (outer shell) thicknesses, and infill densities (Table 1). The tablets were printed at a nozzle temperature of 190 °C. The other settings used for 3D printing were as follows: bed temperature, 60 °C; nozzle traveling speed, 50 mm/s; layer height, 0.10 mm; and printing speed, 50 mm/s.

The structural parameters of a dosage form that were altered in FDM 3D printing were shell thickness, wall thickness (outer shell) and infill density. The shell can be defined as the total width of the perimeter of the dosage form, whereas the wall was a part of the shell that had different infill patterns and compact structures compared to the inner core. Alteration in infill density changes the porosity of the structure of the dosage form. The wall has the same composition as that of the shell, but the printing pattern is different from the shell. Firstly, pure HPC filaments were used to print the hollow tablets with four different shell thicknesses (0.8, 1.2, 1.6, and 2.0 mm) as shown in Figure 2A. To assess the lag time, in vitro release studies were conducted for floating tablets of plain HPC and HPC with different concentrations of ethyl cellulose (0.5 to 10 w/w%). The developed tablets with 0.5% EC exhibited a desired lag time of 6 h. Secondly, to assess the effect of wall thickness and% infill density of the shell on the drug release profiles, tablets with three different wall thickness (outer shell) (0, 0.8, and 1.6 mm) as shown in (Figure 2B) and three

different % infill densities (50, 75, and 100) as shown in (Figure 2C) were printed using the filament containing 0.5% EC. The impact of infill density can only be assessed without a wall. So, a wall thickness of 0 mm was used while printing the tablets with different infill densities.

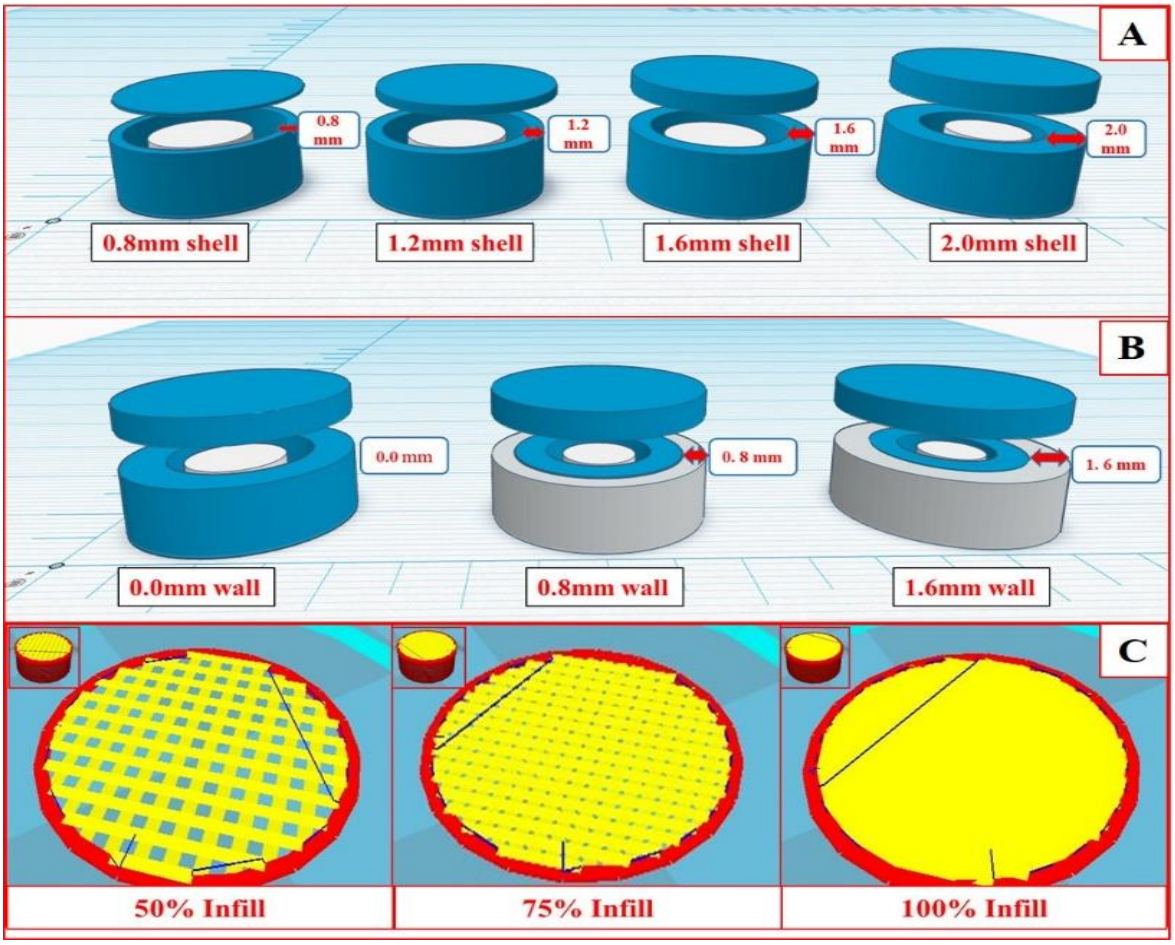

Fig. 3.2. Graphical images of the floating tablets with different shell thickness (A), wall thickness (B), and infill density (C).

3.3.6 Loading capacity and buoyancy of the 3DP floating tablets

The printed tablets should remain buoyant on the gastric fluid in the stomach until the pulse release of the drugs occurs. Theoretically, an object can float when the buoyancy force exerted by the fluid is more than the opposite force by gravity (Archimedes' principle) i.e. if the total force acting vertically on the object is positive. To attain this, the total density of the dosage form should be less than the density of the gastric contents (reported as ~1.004 g/ml) . Based on this principle,

the maximum amount of the drug that can be loaded in the proposed floating system and can remain buoyant on the gastric fluid was calculated.

3.3.7 In vitro floating study and refloating ability

The in vitro floating study of the 3D printed floating tablets was performed using a United States Pharmacopeia (USP II) dissolution test apparatus (Hanson SR8-plus™; Hanson Research, Chatsworth, CA, USA). The media was 900 mL of 0.1 N HCl maintained at 37 ± 0.5 °C and the paddle speed was set at 50 rpm. To determine the re-floating ability of the printed tablets, tablets were immersed in the dissolution medium for 5 s per hour using a glass rod during the floating study. Test was performed in triplicate. To obtain the images of the floating tablets clearly, the tablets were transferred to 500 mL glass beakers filled with the dissolution media and the photographs were captured at 0, 2, 4, and 6 h.

3.3.8 Scanning electron microscopy (SEM)

The surface morphology of the extruded filaments and 3D printed floating tablets were studied with a JOEL JSM 5610LV scanning electron microscope (SEM) (JOEL, MA, USA) with an accelerating voltage of 5 kV. All the samples were placed on the SEM stubs and adhered by using double-adhesive tapes. The samples were sputter-coated with gold under an argon atmosphere using a Hummer 6.2 Sputter Coater (Ladd Research Industries, Williston, VT, USA) prior to imaging.

3.3.9 In vitro drug release study

The drug release characteristics of the 3D printed floating tablets were determined using a United States Pharmacopeia (USP II) dissolution test apparatus (Hanson SR8-plus™; Hanson Research, Chatsworth, CA, USA). The dissolution media was 900 mL of 0.1 N HCl maintained at

37 ± 0.5 °C, and the paddle speed was set at 50 rpm. The samples were collected at the pre-determined time intervals and analyzed for drug content using a UV/VIS spectrophotometer (GENESYS 180, Thermo Scientific) at a wavelength of 272 nm. The calibration curve of y = 0.0556x + 0.008 was acquired with an r^2 value of 0.9996. Each test was carried out in triplicate and the collected data were plotted as percentage cumulative drug release versus time.

3.3.10 Statistical Analysis

Statistical analysis was performed by one-way analysis of variance (ANOVA) with Student-Newman-Keuls post-hoc testing using GraphPad Prism 5 software (GraphPad Software, CA, USA) with $p \leq 0.05$ as the level of significance.

3. 4. Results and Discussion

3.4.1 Thermal analysis of the polymers

The thermal degradation behaviors of HPC and EC are analyzed using thermogravimetric analyzer. From the results and literature reports, it was observed that the percentage loss in the mass was <1% at the temperature (190° C) used for 3D printing of the tablets. A significant mass loss of the polymers was observed at temperatures of >250°C, implying that the polymers were stable during the HME and 3D printing processes.

3.4.2 Filament preparation and characterization

Different pharmaceutical-grade polymers were recently investigated for FDM 3D printing of the tablets for various applications. From the available pharmaceutical-grade polymers suitable for FDM 3D printing, HPC was utilized for the preparation of domperidone sustained release intragastric floating tablets. In this study, HPC was chosen for fabrication of the filaments required as feedstock materials for the development of 3D printed floating pulsatile tablets. In the

preliminary studies, EC was added at different concentrations (10%, 5%, 2.5%, and 1%) to HPC to prolong the lag time for the pulsatile drug release characteristics. After all the EC concentrations were studied, the lag time observed was > 8 h. To attain the desired 6 h lag time, 0.5% of EC was utilized in the formulation.

During the HME process, the filaments exiting the extruder die were coiled in irregular shapes and were difficult to process through the 3D printer. Therefore, a conveyor belt was used to straighten the filaments for easy loading into the 3D printer. After solidification, the filaments were coiled and stored in a desiccator to prevent any moisture uptake. The filaments that absorbed moisture became soft and squeezed between the feeding gears of the 3D printer. This is because, after moisture absorption, the flexibility of the filaments increased, preventing the melted material from pushing through the heater. Further, the inflow of materials from the printer nozzle was irregular.

After fabrication of the filaments using the HME technique, the mechanical properties of these extruded filaments were tested using a texture analyzer and compared with those of the commercially available polylactic acid (PLA) filaments having optimum mechanical properties suitable for FDM 3D printing. For a filament to be considered suitable for FDM 3D printing, it should not either break or curved aside by the feeding gears during the feeding process which might result in an inadequate flow of materials through the nozzle. If the filament is too brittle it may break by the gears and if it is too flexible it may be curved away from the feeding gears due to the inability to push the materials through the narrow 0.4 mm nozzle of the 3D printer. For this reason, there should be a balance between the brittleness and the flexibility of the filaments.

Even though PLA is considered as reference material for comparing the mechanical properties of the filaments in 3D printing, it is interesting to note that filaments with a lower stiffness (breaking stress and force) than the PLA filament were good enough for the FDM 3D printing process. This

may be due to a variation in the force applied by the gears of the different 3D printers during feeding of the filaments into the 3D printer. In this study (Figure. 3), the force required to create a 35% deformation in the shape of the filament was considered as the maximum force which the filaments could withhold during the feeding process without any breaking or squeezing phenomenon in the feeder. Pure HPC and HPC+ EC require a lower force of 8500 g and 7409 g, respectively, as compared to that of the reference material PLA (25630 g). But these filaments did not show any breaking or squeezing problems during the printing process which resulted in the fabrication of high-quality floating tablets.

In a study conducted by Chai et al., 2017, the authors developed intragastric sustained release floating tablets of domperidone using HPC EXF as matrix polymer for fabrication of filaments. The authors used 10% (w/w) domperidone in filament composition. The fabricated filaments exhibited desired mechanical properties suitable for FDM 3D printing. Similar results were observed in the current study. In the earlier study, filaments fabricated using HPC EF and HPC HF grades with 30% paracetamol were not suitable for FDM 3D printing [32]. The filaments produced using both HPC EF and HPC HF were too soft. This may be due to relatively high drug load of 30% (w/w) paracetamol which acted as a plasticizer and softened the filaments. These studies indicate the significance of drug loading and properties of drug in the fabrication of filaments to be utilized in FDM 3D printing.

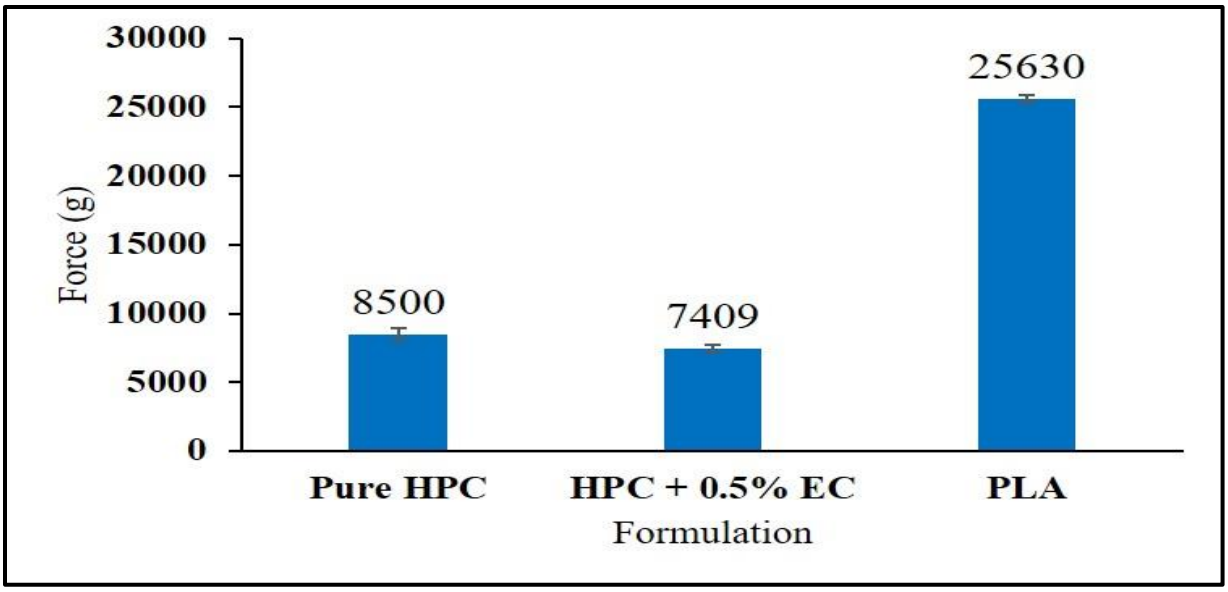

Fig. 3.3. Force values of stiffness test of the hot-melt extruded filaments (error bars represent mean ± S. D).

3.4.3 Physical properties of the compressed tablets

After performing preliminary experiments with different ratios of theophylline and other ingredients, the composition [theophylline (57% w/w), croscarmellose sodium (8% w/w), microcrystalline cellulose (34% w/w), and magnesium stearate (1% w/w)] was selected to prepare immediate-release theophylline tablets. All the compressed theophylline tablets demonstrated acceptable uniformity in weight (175 ± 5.8 mg), thickness (2.9 ± 0.16 mm), and hardness (4.2 ± 0.70 kp). The disintegration time was < 1 min and the tablets showed 100% drug release within 30 min.

3.4.4 3D printing of the floating tablets

The physical properties of all the printed floating tablets are enumerated in Table 1. 3D printing of the floating pulsatile tablets was achieved in three steps (Figure 4). In the first step, 80% of the tablet shells were printed and the printer was paused. In the second step, the directly compressed core tablets were placed in the 80% printed shell and the final printing was resumed

to form a completely sealed floating tablet. This process resulted in the printing of tablets without any structural defects. The thicknesses of the top and bottom were the same as the shell thickness of all the prepared tablets. The tablets printed without any wall had rough surfaces and structural defects in some of the tablets, whereas the surfaces of the tablets with walls were smooth and no structural deformities were observed during the printing process

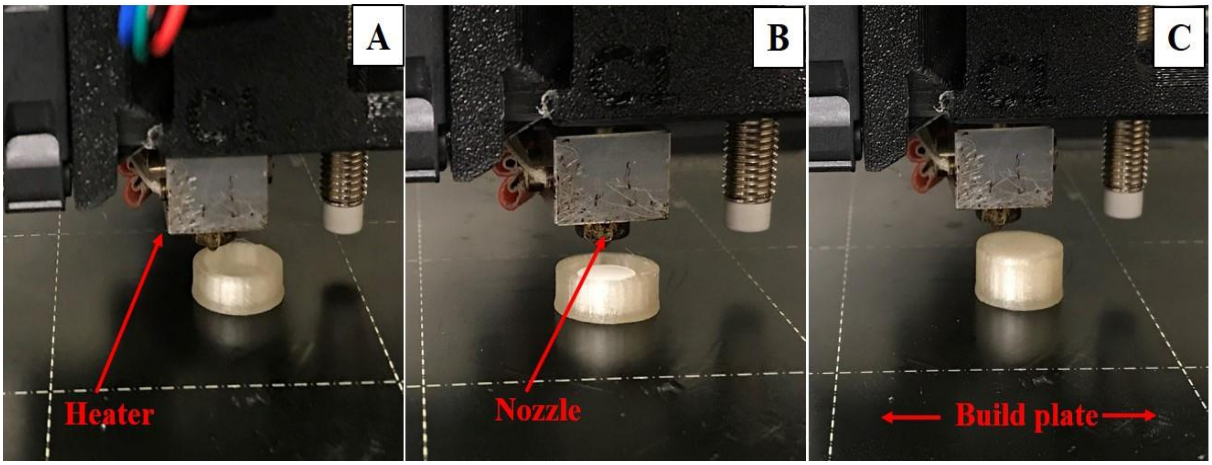

Fig. 3.4. Eighty percent of the printed empty shell of a floating tablet (A), placement of a compressed tablet in the shell (B), and a completely sealed floating tablet (C).

Table 3.1. Physical properties of the 3D printed floating tablets.

Filament 1 [100%[w/w] HPC]					
Shell thickness [mm]	Wall thickness [mm]	Infill density [%]	weight [mg]	Density [mg/mm^3]	Floating duration [h]
0.8 mm	0.8 mm	100	633±11	0.548	1.5±0.21
1.2 mm	0.8 mm	100	775±12	0.671	3.0±0.16
1.6 mm	0.8 mm	100	868±19	0.752	3.5±0.08
2.0 mm	0.8 mm	100	1088±7	0.942	4.0±0.12
Filament 2 [0.5%EC[w/w], 99.5% HPC]					
Shell thickness [mm]	wall thickness [mm]	Infill density [%]	weight [mg]	density [mg/mm^3]	Floating duration [h]
2.0 mm	1.6 mm	100	1086±7	0.941	6.0±0.09
	0.8 mm	100	1081±11	0.935	5.0±0.13
	0.0 mm	100	1080±16	0.935	4.5±0.26
		75	902±8	0.781	2.0±0.22
		50	649±10	0.562	0.5±0.19

3.4.5 Loading capacity and buoyancy of the 3D floating tablets

For a tablet to remain buoyant in the gastric fluid,

$F_{Buoyancy} \geq F_{Gravity}$. (1)

The above statement (1) can also be represented as follows:

$\rho_L V_{max} g \geq (m_s + m_t) g$, (2)

where ρ_L is the density of gastric fluid, V_{max} is the maximum volume of liquid displaced (i.e. the volume of floating pulsatile tablet, Vt), g is the acceleration due to gravity, ms is the mass of shell, and mt is the mass of the compressed tablet. The equation (2) is simplified as equation (3):

$\rho_L V_t \geq (m_s + m_t)$, (3)

Where ρ_L is the density of the gastric fluid i.e. 1 g/cm3, and mass of shell (ms) + mass of compressed tablet (mt) is the total mass of the floating tablet (Mt). So, equation (3) was further simplified as equation (4) as follows:

$(\rho_L V_t) - m_s \geq m_t$. (4)

The volume of the floating tablet (Vt) can be calculated from its dimensions. The optimized floating tablet shell had a weight of 913 mg and a volume of 1155 mm3. So, the maximum weight of the compressed core tablet that can be accommodated was 242 mg. In our study, we used a compressed core tablet having a total weight of 175 mg which is equivalent to 100 mg of theophylline. By optimizing the composition of the core compressed tablets for an immediate-release profile, any drug that is a suitable candidate for a floating pulsatile release system can be delivered with this proposed pulsatile floating tablet.

3.4.6 Floating and refloating abilities of the printed tablets

All the tablets placed in the dissolution media floated immediately without any lag time. The floating abilities of the printed tablets highly correlated with their densities as reported in the previous literature [28]. Tablets with a density of > 1 mg/mm3 sunk to the bottom of the dissolution vessels. The density of the printed tablets ranges from 0.548−0.941 mg/mm3. Tablets with high shell thickness and high infill had higher densities. No difference in the density was observed between the tablets with various wall thicknesses with 100% infill density ($P < 0.005$). When the tablets were immersed into the dissolution media to see the refloating ability, they rose to the top of the dissolution vessel immediately without any lag time. All the tablets showed good refloating abilities without any loss of the structural integrities. The images of the floating tablets obtained at different time points during the dissolution study are shown in Figure 5.

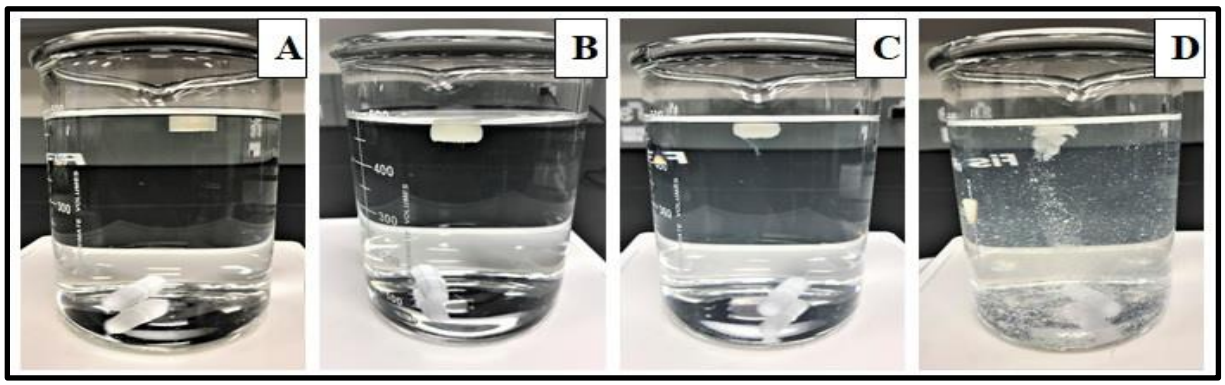

Fig. 3.5. Images of the floating tablets taken at different time points during the dissolution study in 0.1N HCL: 0 h (A), 2 h (B), 4 h (C), and 6 h (D).

3.4.7 Surface morphology

The surface morphology of the extruded filaments, cross-sectional structure, and surface of the floating tablets are shown in Figure 6. The surfaces of the extruded filament were smooth and homogeneous without any deformities suggesting suitability for 3D printing. The filaments having rough or irregular surfaces will not feed smoothly into the 3D printer and will result in irregular shaped tablets. The cross-sectional structure of the floating tablets showed multiple single

layers printed sided by side to form the shell. The surface of the 100% infill 3D printed tablets showed close adjacent layers without any gaps.

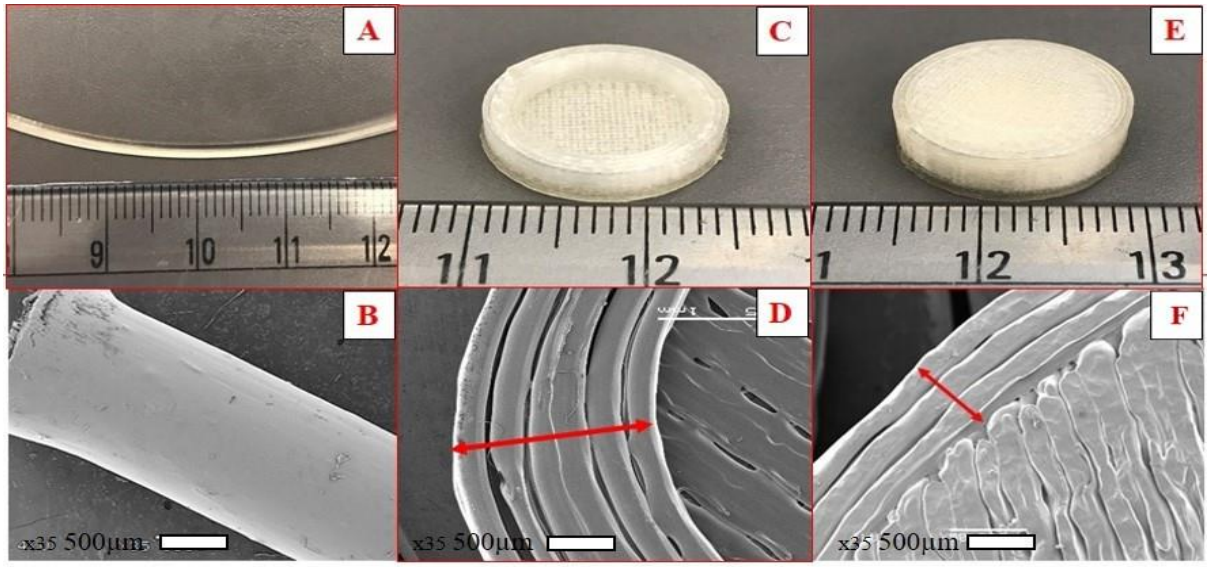

Fig. 3.6. Digital images and representative SEM images of the HME filament (A and B), the cross-sectional structure of the floating tablet showing shell (C and D), and surface morphology of a 100% infill 3D printed tablet (E and F).

3.4.8 In vitro dissolution study

The dissolution behavior of the 3D printed floating tablets is shown in Figure 7. From the dissolution data, it was observed that both the tablet geometry and addition of EC into HPC had significant effect on the drug release profiles ($P < 0.05$). The tablets with higher shell thicknesses had integrity for a longer duration of time before the pulse release of API into the dissolution media as compared to the lower thickness (Figure 7A). The tablets having a shell thickness of 2.0 mm (highest) demonstrated pulse release at the end of 4±0.12 h, whereas those with a shell thickness of 0.8 mm (lowest) showed drug release in 1.5±0.21 h. The tablets with a shell thickness of 1.2 mm and 1.6 mm showed a lag time of 3±0.16 and 3.5±0.08 h, respectively, before complete drug release. Similar results were reported in the literature on the effects of shell thickness. In a previous study conducted by Maroni et al., the authors printed two-compartment capsular devices, each

compartment with different thicknesses and reported that the duration of the lag phase for the pulse release of drugs increased proportionally with an increase in the compartment thickness (Maroni et al., 2017). This phenomenon can be caused by a higher shell thickness that prevented the entry of the dissolution media into the core for a longer time. The addition of EC to the formulation increased the threshold time for complete drug release (Figure 7B). The tablets with 2.0 mm shell thickness, which had an EC of 0.5%, showed pulse release at the end of 5±0.13 h.

To assess the effect of the wall thickness and infill density of shell on the pulse release of drug, tablets with three different wall thicknesses (0.0, 0.8, and 1.6 mm) and three infill densities were studied (50%, 75%, and 100%). The tablets with higher wall thicknesses prevented the entry of the dissolution media more effectively than those with low wall thicknesses. This is attributed to the closed compact structure of the wall. This observation was consistent with the results of a previous study [34]. The tablets with 100% infill densities demonstrated pulse release at the end of 4.5±0.26 h, followed by 75% infill (2±0.22 h) and 50% infill (0.5±0.19) (Figure 7C). A higher porosity of lower infill density had a higher surface area and allowed easy entry of the dissolution media into the core, resulted in a faster release of API. Yang et al. 2018, and Chen et al. 2020, who used FDM 3D printing for the development of controlled release dosage forms, reported that a higher fill density caused a reduction in the total surface area and resulted in a slower drug release from the dosage forms.

All the prepared floating tablets exhibited a pulse release of drug with different threshold times varying from 30 min to 6 h. The tablets with specific geometrical structure (2 mm shell, 1.6 mm wall, 100% infill) with 0.5% EC (Figure 7D) were considered optimized formulations for pulsatile release of drugs after 6 h for effective chronotherapeutic treatment of asthma.

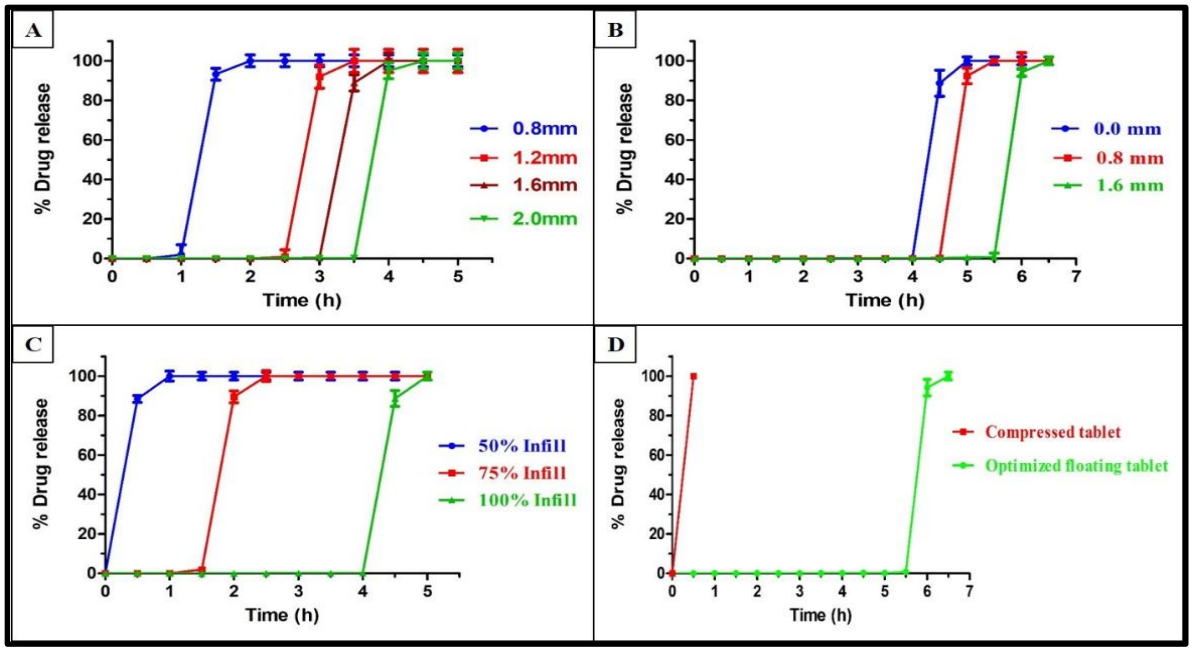

Fig. 3.7. *In vitro* release profiles of the floating tablets with different shell thicknesses in 0.1N HCl (A), different wall thicknesses (B), different fill densities (C), and optimized floating tablets and compressed tablets (D). (error bars represent mean ± S. D).

3.5 Conclusions

Floating pulsatile tablets with the desired lag time for pulse release of theophylline were successfully developed with the proposed HME coupled 3D printing technique. The geometrical properties of the tablets (shell and wall thickness and infill density) and EC showed significant effect on the lag time. Thus, the lag time can be varied from 30 min to 6 h based on the requirements. The proposed floating pulsatile system showed a high potential to deliver drugs that need high residence time in the stomach and the pulsatile release of theophylline. This strategy reduces unwanted adverse effects and improves patient compliance. In addition, thermolabile drugs can be delivered through this system as the inner core tablet is not exposed to high temperatures involved in the FDM 3D printing process. In conclusion, HME coupled 3D printing is a novel and potential technique to develop low-cost customized drug dosage forms for

personalized pharmacotherapy. However, dosage forms fabricated using FDM 3D printing technology needs to overcome the challenges in terms of regulatory concerns. Therefore, these floating systems need to be further assessed in in-vivo conditions to demonstrate the suitability for patient use.

CHAPTER 4

Development of sustained release Gastroretentive floating tablets using HME coupled 3D printing: A Quality by Design approach

4.1 Introduction

Though oral drug administration is the most preferred route of administration for dosage forms, due to physiological variations such as unpredictable gastric emptying time and transit time, oral absorption has become unsatisfactory. And short gastric emptying will result in incomplete drug release from the dosage form leading to poor therapeutic effect (Chai et al., 2017). And for several drug molecules (e.g. baclofen, pranlukast hydrate, metformin HCl), upper part of the gastrointestinal tract is the main site for absorption. Some drugs are prone to degradation in colonic environment (ranitidine, captopril etc.). Drugs that have shorter half-lives, recurrent dosing is necessary to attain required therapeutic concentrations. To overcome all these limitations of oral drug delivery, a drug delivery system with increased gastric retention and sustained release properties is necessary (Sugihara et al., 2014, Nayak et al., 2010, Kesarla et al., 2015).

Several approaches are used by researchers to increase the gastric retention of dosage forms including low density systems, high density systems, expandable systems, bio adhesive systems, raft forming systems, super porous hydrogel systems, magnetic systems, and ion-exchange resin systems. Among all these approaches low density systems (floating systems) were considered as

most practical and extensively studied gastroretentive dosage forms. Floating dosage forms had bulk density less than gastric fluid (1.01 g/cm^3) and hence float on gastric region, avoiding gastric emptying (Lopes et al., 2016, Tripathi et al., 2019).

Quality by design (QbD, according to the ICH Q8(R2) document (2009) is defined as a systematic approach to development that begins with predefined objectives and emphasizes product and process understanding based on sound science and quality risk management. Pharmaceutical products should be designed in such a way that, patient's safety and product's efficacy and performance are maintained. Quality target product profile (QTPP) are defined based on these characteristics.

In this study, hot melt extrusion was combined with fused deposition modeling 3D printing to prepare the floating tablets. Hot melt extrusion was used to manufacture the cylindrical filaments which were used as feedstock material for 3D printing. Acetaminophen was used a model drug. HPMC was selected as matrix polymer which was previously used by several researchers in FDM 3D printing for formulation of various dosage forms. Ethyl cellulose was included in the formulation to sustain the drug release from the dosage forms. A quality by design approach was employed in the present study to understand the effect of both formulation and process parameters on the in vitro drug release profiles of the 3D printed floating tablets.

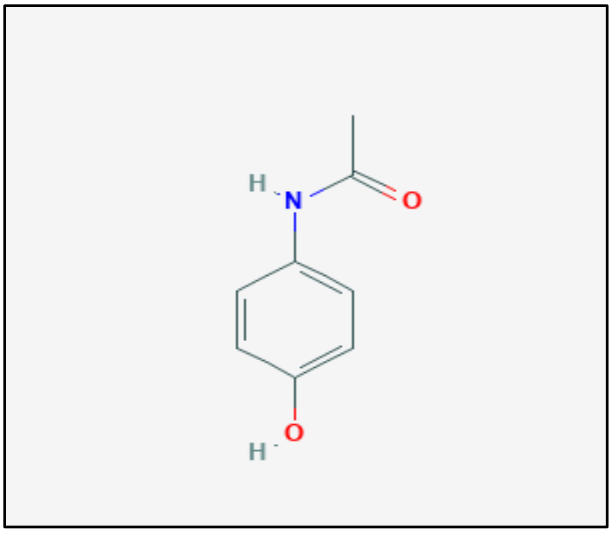

Chemical structure of Acetaminophen

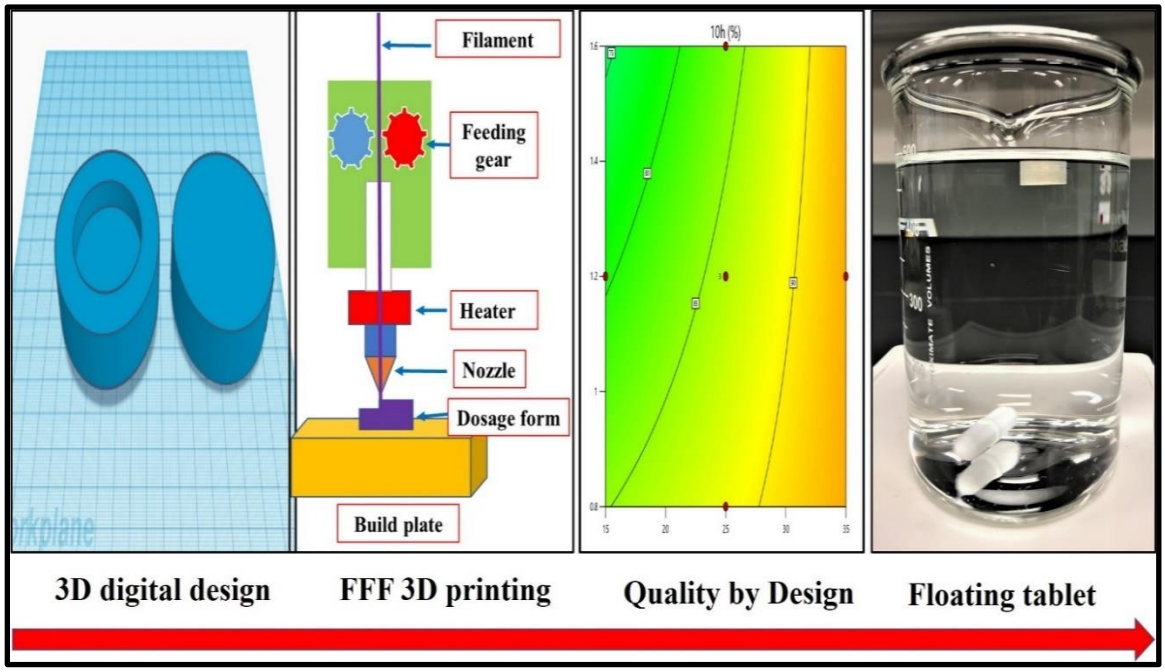

Fig. 4.1. Graphical representation of development of sustained release floating tablets with FDM 3D printing.

4.2 Materials

Acetaminophen (APAP) was purchased from spectrum chemical (New Brunswick, NJ, USA). Hydroxypropyl methylcellulose (HPMC E5), Benecel^{TM} HPMC E5, Aqualon^{TM} EC N14

were donated by Ashland Inc. (Covington, KY, USA). All other chemicals used in this study were of analytical grade.

4.3 Methods

4.3.1 Hot melt extrusion processing

All the formulations used for extrusion were shown in Table. 1. The formulations were homogeneously blended using Maxiblend™ (GlobePharma, New Brunswick, NJ, USA) at 25 rpm for 15 minutes and were extruded using 11mm twin screw co-rotating extruder (Thermo Fisher Scientific, Waltham, MA, USA). A round 1.5mm die was used for extrusion of filaments. The temperature used for extrusion was 160 °C and screw speed was 100 rpm for all the formulations and torque observed inside extruder was within the limit where extruder can function smoothly. A conveyor belt was used to straighten and obtain the uniform filaments. The filaments obtained were coiled and stored in a desiccator to avoid moisture uptake and used during 3D printing of floating dosage forms.

Table.4.1 Formulation and process parameters of hot melt extrusion processing

Formulation No.	APAP (%)	HPMC (%)	EC (%)	Temp (°C)	Torque (%)
1	15	85	0	160	55-60
2	15	65	20	160	50-55
3	15	55	40	160	40-45
4	25	75	0	160	35-40
5	25	55	20	160	30-35
6	25	35	40	160	25-30
7	35	65	0	160	20-25
8	35	45	20	160	10-15
9	35	25	40	160	5-10

4.3.2 Filament characterization

4.3.2.1 Repka-Zhang test

Mechanical properties of the extruded filaments were determined using a Texture Analyzer (TA-XT2i analyzer, Texture Technologies, Hamilton, MA, USA).The Filaments were cut into length of 5 mm each and placed on the bottom flat surface of the texture analyzer. The top blade part of the texture analyzer was moved down until it penetrates into the filament (0.6mm) to create a 35% deformation in the shape of the filament and the force/breaking stress required to deform the filament were measured.

4.3.3 Quality by Design experiments

A response surface method, three-factor, three-level Box–Behnken design was applied for the optimization of sustained release floating tablets. The low and high levels of factors were decided based on previous preliminary experiments. The medium levels were set as the midpoint of low and high levels. The Design of Experiments (DoE) independent variables and formulations suggested by software (Design-Expert^{R} version 11) were given in Table 2. A total of 15 experiments were suggested by the software. Cumulative drug release (%) at 2h, 6h and 10h were chosen as responses. The dissolution data obtained was processed using (Design-ExpertR version 11) and analyzed to see the effect of input parameters on output parameters.

Table. 4.2. DoE independent variables and the experiments suggested by the Design-Expert software

Variables	Unit	Lower limit	Upper limit
Drug load	% (w/w)	15	35
Shell thickness	mm	0.8	1.6
EC	% (w/w)	0	40

Run. No	APAP (%)	Shell thickness (mm)	EC (%)
1	25	1.2	20
2	25	1.2	0
3	35	1.6	0
4	15	1.6	40
5	35	1.6	40
6	35	1.2	20
7	15	0.8	0
9	35	0.8	0
10	15	1.6	0
11	25	1.6	20
12	25	1.2	40
14	15	0.8	40
15	35	0.8	40
16	15	1.2	20
17	25	0.8	20

4.3.4 Fused deposition modeling (FDM) 3D printing.

The tablets were designed as hollow cylindrical objects to decrease density and float in gastric medium, using Autodesk® Tinkercad™ free online software (Autodesk, CA, USA) as shown in Figure 1. Combining both these digital files and previously extruded filaments, the

gastroretentive floating tablets were prepared using FFF based 3D printer (Prusa i3 3D desktop printer, Prusa Research, Prague, Czech Republic). All the tablets were printed at nozzle temperature of 190 ˚C and bed temperature was maintained at 60 ˚C. The parameters for printing were as follows. Nozzle diameter: 0.4mm, layer thickness: 0.1mm, print speed: 60mm/sec, infill pattern: Lines, top/bottom thickness:1mm. Time taken printing of each tablet was in between 5-6 minutes.

4.3.5 Differential Scanning Calorimetry

DSC studies were performed for APAP, HPMC, EC, physical mixtures and formulations using Discovery DSC 25 (TA Instruments DSC, New Castle, DE, USA), coupled with a RCS90 cooling device. All samples weighed approximately 5-10 mg and were sealed in Tzero aluminum pan. The samples were equilibrated under nitrogen gas for one minute at 25 °C and then heated at a rate of 10 °C/min under an inert nitrogen purge of 50 mL/min. The thermograms were analyzed for the amorphous or crystalline nature of drug.

4.3.6 Drug content of filaments and tablets

Tablets or filaments equivalent to 100mg of APAP were crushed and transferred to 100 mL of volumetric flask, 50 mL of ethanol was added, and the volumetric flasks were sealed with parafilm and sonicated for 30 minutes (Branson 2510, Branson Ultrasonic Corp., Danbury, CT, USA). Finally, the volume of the flasks was made up to 100 mL. Samples were centrifuged at 16000 rpm for 15 min, the supernatant was collected and diluted with 0.1N HCl and analyzed separately for the drug contents using UV- spectrophotometer at 243 nm. The samples were analyzed in triplicate.

4.3.7 *In vitro* dissolution studies and floating ability

The drug release characteristics of the 3D printed floating tablets were determined using a United States Pharmacopeia (USP II) dissolution test apparatus (Hanson SR8-plus™; Hanson Research, Chatsworth, CA, USA). The dissolution media was 900 mL of 0.1 N HCl maintained at 37 ± 0.5 °C, and the paddle speed was set at 50 rpm. The samples were collected at pre-determined time intervals and analyzed for drug content using a UV/VIS spectrophotometer (GENESYS 180, Thermo Scientific) at a wavelength of 260 nm. Each test was carried out in triplicate and the collected data were plotted as percentage cumulative drug release versus time. The tablets were also assessed for floating ability and lag time in the same dissolution media.

4.3.8 Scanning electron microscope

The surface morphology of the 3D printed floating tablets (one formulation with EC and one without EC) were studied with a JOEL JSM 5610LV scanning electron microscope (SEM) (JOEL, MA, USA) with an accelerating voltage of 5 kV. All the samples were placed on the SEM stubs and adhered by using double-adhesive tapes. The samples were sputter-coated with platinum under an argon atmosphere using a Hummer 6.2 Sputter Coater (Ladd Research Industries, Williston, VT, USA) prior to imaging. The images were taken 200x resolution to observe the surface of tablet precisely.

4.3.9 Statistical analysis

Analysis of variance (ANOVA) was used to analyze data from the experimental design. At $p < 0.05$, the differences in data were considered statistically significant.

4.4 Results and discussion

4.4.1 Hot melt extrusion processing

The process of hot melt extrusion was smooth, and the torque observed inside the barrel was less than the maximum limit for alarm. The torque observed insider the extruder barrel was between 5-60%. The torque reduced as the (%w/w) drug increases in the formulation. At 160°, APAP was acting as plasticizer and this resulted in the reduction of torque as % of APAP increased in the formulation. The filaments obtained from all the formulations were homogeneous and uniform in diameter.

4.4.2 Filament characterization

Hot melt extruded filaments which will be used as feedstock material in FDM 3D printing should possess suitable mechanical, rheological, and adhesive properties to produce dosage forms of high quality. Flexibility and brittleness of filaments are two key mechanical properties that are used to assess the suitability of filaments for FDM 3D printing. Currently available poly lactic acid (PLA) filaments possess ideal mechanical, rheological and adhesive properties for FDM 3D printing and is being used as a reference material by several researchers for predicting the suitability of pharmaceutical grade polymers for printing.

Filaments should have a balance between flexibility and brittleness for successful feeding through FDM 3D printer. Brittle filaments are hard to be loaded into the printer head and can easily broke by feeding gears and this may lead to the blockage of the nozzle. Filaments which are too flexible

will be squeezed between feeding gears of printer resulting in failure to push the material through the printer nozzle

Zhang-Repka test was used to assess the mechanical characters of the extruded filaments and compared with the commercially available poly lactic acid (PLA) filament. All the filaments tested in this study showed force above 18000 g/mm^2, compared to PLA of 25600 g/mm^2. But all the filaments showed desired mechanical characteristics for 3D printing. Though the stiffness of the extruded filaments were not exactly equal to the stiffness of commercially available filament, the filaments did not show any signs of squeezing phenomenon inside the feeding gears, implying the filaments had minimal stiffness required for 3D printing of dosage forms.

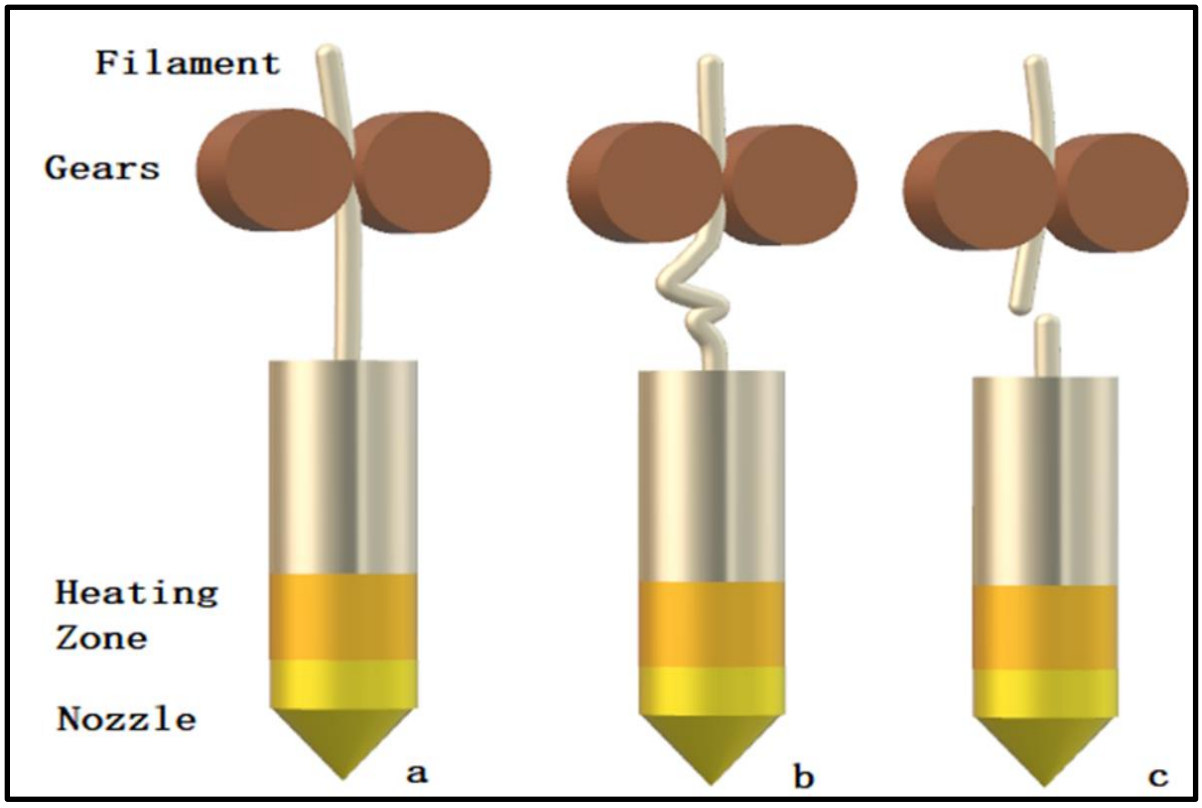

Fig. 4.2. Graphical image showing the behavior of filaments during FDM 3D printing process with different mechanical properties a) optimum b) flexible c) brittle

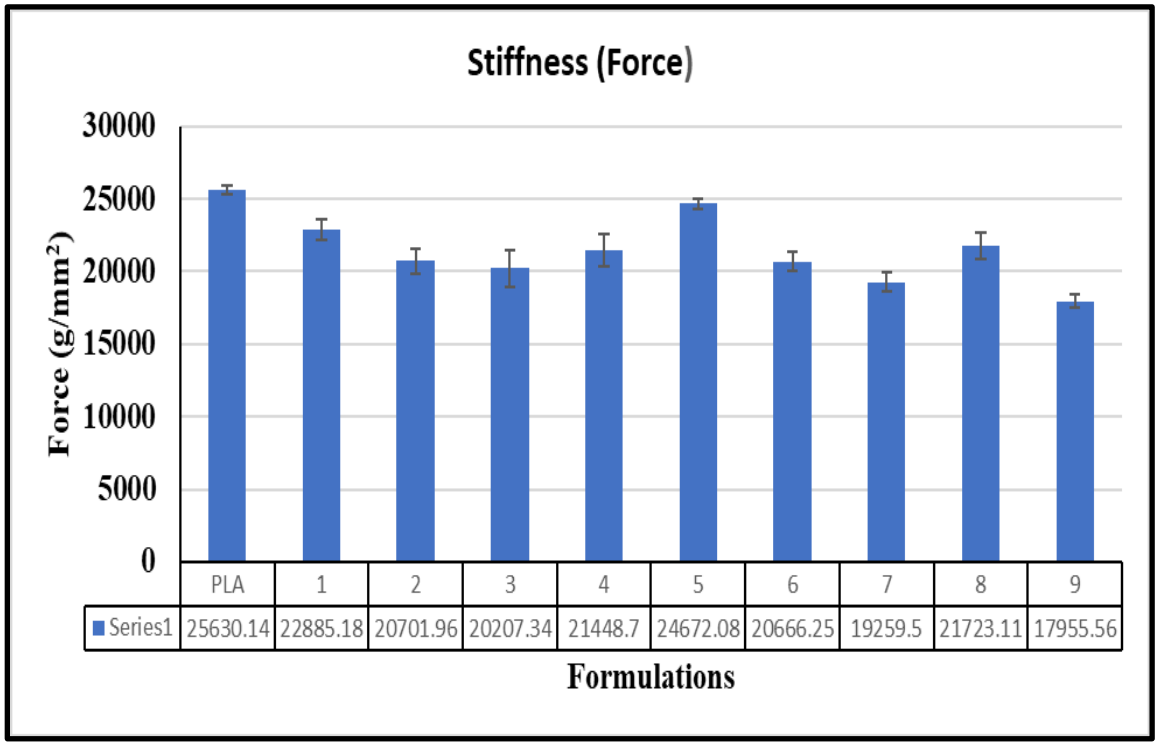

Figure 4.3. Stiffness values of all the extruded filaments analyzed by Repka-zhang test

4.4.3 3D printing of floating tablets

The extruded filaments were loaded into 3D printer and combined with 3D digital models to print the floating tablets. The dimensions of the tablets were (d=12.4mm, h=5mm) and the shell thickness was varied between 0.8 to 1.6mm. All the tablets had bulk density less than 1.01 g/cm^3, less than the density of gastric contents and hence were able to float on dissolution media.

4.4.4 Differential scanning Calorimetry

The thermogram of APAP showed sharp endotherm peak around 165 °C corresponding to its melting point. The endotherm disappeared in all the other formulations, implying APAP converted to amorphous during the HME process. The intense shear generated by the three mixing zones of the standard screw configuration converted the crystalline APAP into its amorphous form. Small endotherms with very little intensity can be seen in formulations with 35% drug loading. This might be due to presence of small amount of crystalline APAP in the formulations because of higher drug load.

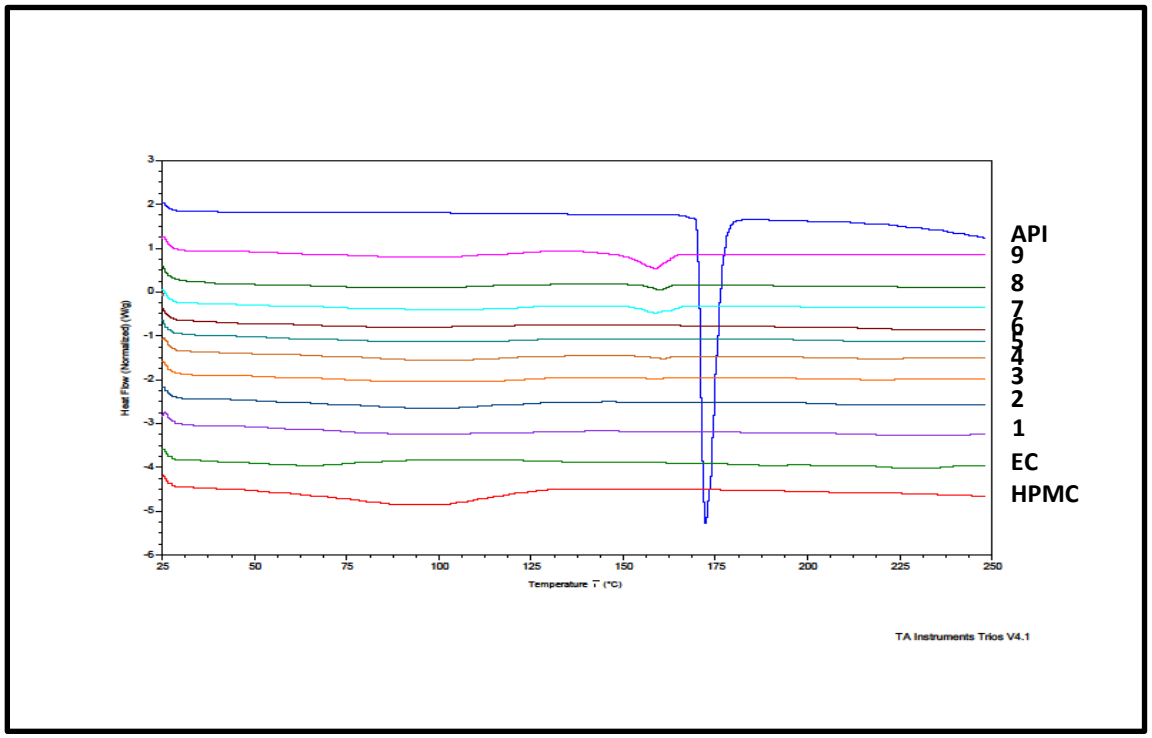

Fig. 4.4. DSC thermograms of pure APA, polymers and all the nine extruded filaments.

4.4.5 In vitro dissolution studies and floating ability

The drug release of the floating tablets sustained for 6-12 hours, for different formulations. The invitro release profiles of all the DoE formulations were shown in Fig. 5. And the % drug

release at 2h, 6h and 10h (dependent factors) were given in table 3. ANOVA was applied to the cumulative drug release profiles and analyzed using Design-Expert^{R} version 11 software to see the effect of dependent factors (predictors) on drug release at 2h, 6h and 10h (responses). The model summaries (linear, two factor interaction and quadratic models) were compared and summarized in Table. 4. If the values of coefficient (β) are positive, it means that there is increase in response variable with one-unit increase in factor considering all the other factors in the equation are constant. All the three factors (APAP%, shell thickness and %EC) had influenced drug release kinetics.

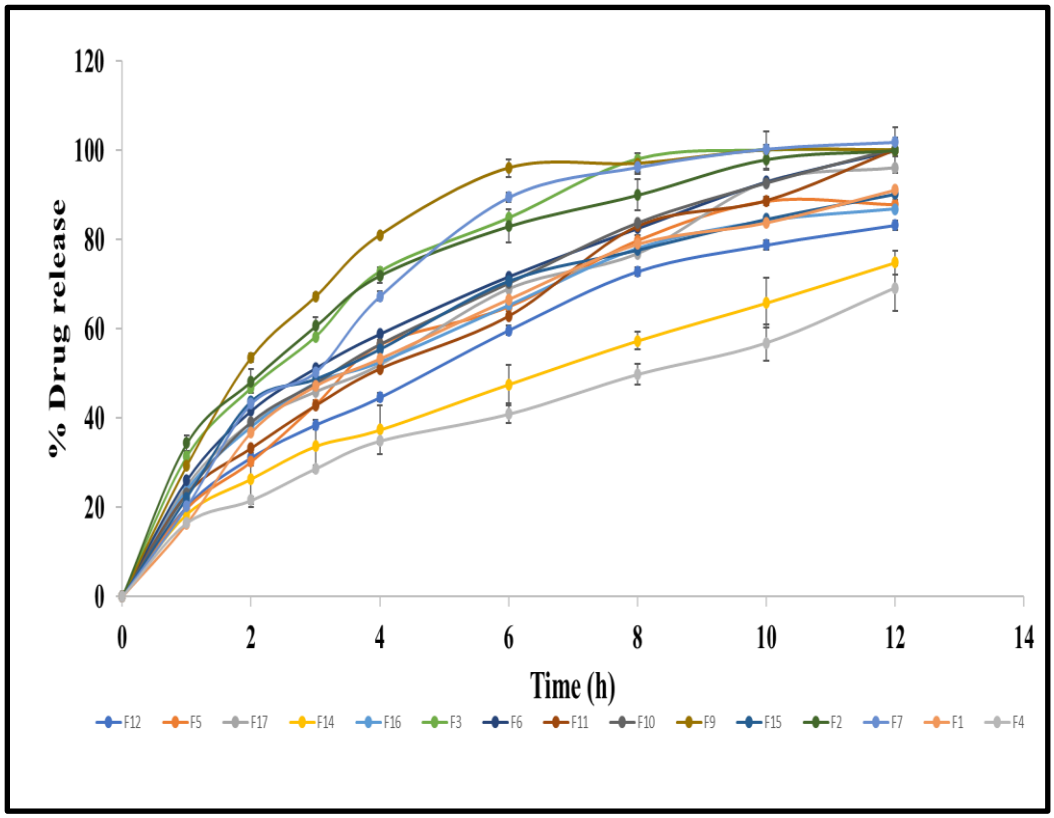

Fig. 4.5. In vitro release profile of sustained release floating tablets in 0.1N HCl.

Table. 4.3 Cumulative drug release values of the all the formulations at 2h, 6h and 10thh.

Run. No	Dissolution (%) 2h	Dissolution (%) 6h	Dissolution (%) 10h
1	36.8	66.6	83.7
2	48.2	83.0	98.0
3	46.7	84.8	100.0
4	21.5	40.9	56.8
5	34.2	65.0	88.6
6	41.6	71.7	93.0
7	43.2	89.4	100.3
9	57.5	96.0	100.0
10	39.1	70.2	92.6
11	33.3	62.8	78.7
12	31.1	59.7	78.8
14	26.4	47.6	65.8
15	43.8	70.7	84.5
16	38.0	65.3	84.1
17	38.9	68.9	92.9

Table 4.4. Model summaries of the QbD experiments

	Dissolution (%) at 2h		Dissolution (%) at 6h		Dissolution (%) at 10h	
	Coefficient	p-value	Coefficient	p-value	Coefficient	p-value
Intercept	**37.45**	**-**	**67.03**	**-**	**81.92**	**-**
A-API	**5.57**	**0.0002**	**7.5**	**0.0002**	**3.77**	**0.0009**
B-Shell thickness	**-3.49**	**0.0027**	**-4.9**	**0.0021**	**-5.56**	**0.0636**
C-EC	**-7.77**	**< 0.0001**	**-13.96**	**< 0.0001**	**-14.5**	**< 0.0001**
AB	**-1.43**	**0.1418**	**1.13**	**0.3591**	**-0.6238**	**0.0983**
AC	**1.02**	**0.2776**	**3.26**	**0.0257**	**2.21**	**0.0053**
BC	**0.0626**	**0.9442**	**2.25**	**0.0923**	**-2.87**	**0.8058**
A^2	**1.89**	**0.2451**	**1.14**	**0.587**	**-4.36**	**0.6255**
B^2	**-1.86**	**0.2518**	**-1.47**	**0.4839**	**-7.12**	**0.5272**
C^2	**1.7**	**0.2911**	**3.96**	**0.0875**	**-4.54**	**0.6767**
Adj. R^2	**0.8991**	**-**	**0.8876**	**-**	**0.7807**	**-**
Pre. R^2	**0.8542**	**-**	**0.8152**	**-**	**0.6120**	**-**
F-Value	**20.28**	**-**	**30.76**	**-**	**16.25**	**-**
Model p-value	**0.0003**	**-**	**< 0.0001**	**-**	**0.0007**	**-**

4.4.5.1 Influence of drug loading

The coefficients of % APAP is positive (5.57) implying that drug dissolution increases with increase in API load and the increase in drug dissolution can be considered significant as the p-value is 0.0002. The effect is greater at 6^{th} hour and least at 10^{th} hour. APAP, is freely water-soluble drug, so as the % APAP increased in formulation, the drug release increased.

4.4.5.2 Effect of EC concentration

Contrary to drug load coefficient of % EC is negative (-7.77 at 2^{nd} hour, -13.96 at 6^{th} hour and -14.5 at 10^{th} hour and p-values less than 0.005 at three time points) implying as %EC increases in the formulation composition, cumulative drug release decreases. EC % and cumulative drug release are inversely proportional in this study. This phenomenon can be explained by the fact that, EC is a hydrophobic and water insoluble polymer, so as % EC is increased in the formulation, it hinders the solubility of floating tablets in dissolution media and hence drug release decreased.

4.4.5.3 Effect of shell thickness

Similar to concentration of EC, shell thickness also had negative coefficient at all three time points but showed significant effect at only 2^{nd} hour (p-value- 0.0027) and 6^{th} hour (p-value- 0.0021), but not significant at 10^{th} hour (p-value- 0.0636). The effect was greatest at 6^{th} hour. The result of decreased drug release with increased shell thickness can be explained by the reason that, Shell has separate fill pattern and denser structure compared to other parts of tablet. So higher shell thickness successfully prevented the entry of dissolution media for longer time and resulted in

reduced drug release. And the phenomenon of shell losing its effect on drug release at 10th hour may be due to the reason that by the end of 10th hour of dissolution testing, the floating tablet started to loose it's integrity and there by the shell structure.

4.4.5.4 Floating ability

All the prepared tablets floated immediately when introduced into dissolution media without any lag time. The tablets were able to float until majority of the tablet matrix was dissolved (Fig. 6). To check the refloating ability, tablets were immersed into the dissolution media for 5 seconds during floating study. All the tablets exhibited refloating ability without losing structural integrity.

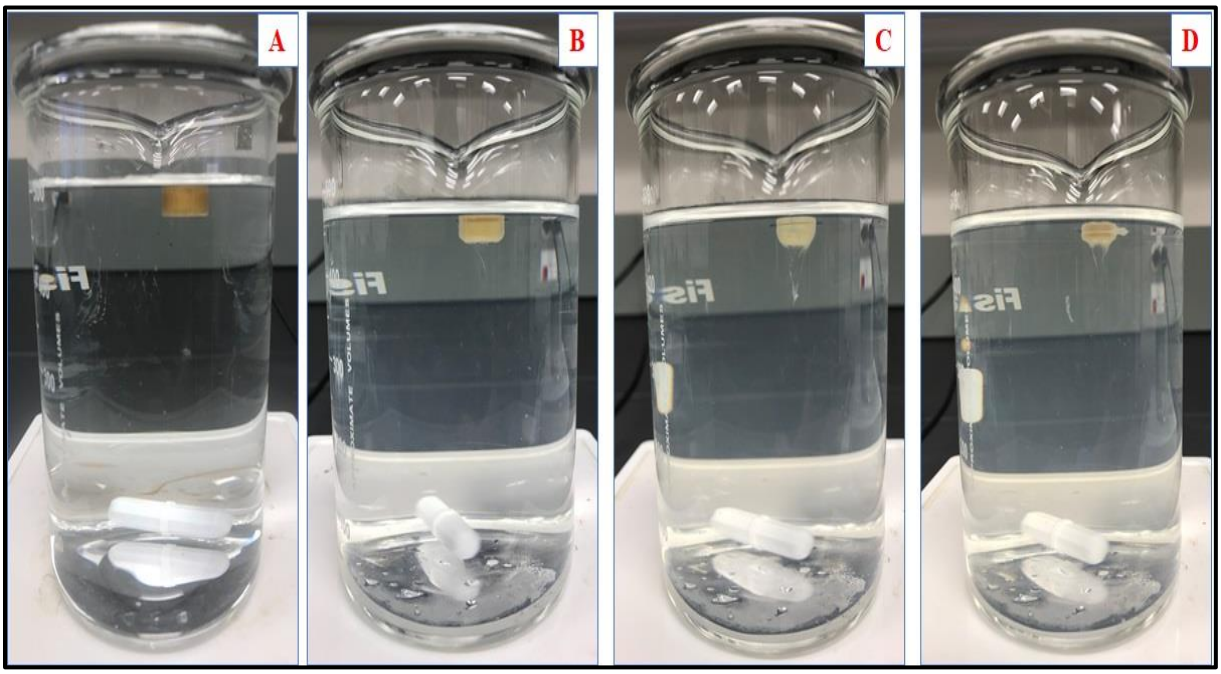

Fig. 4.6. Photographs of 3D printed floating tablets floating in dissolution medium (0.1N HCl). (A) t= 0 h, (B) t= 2 h, (C) t= 4 h and (D) t= 8h.

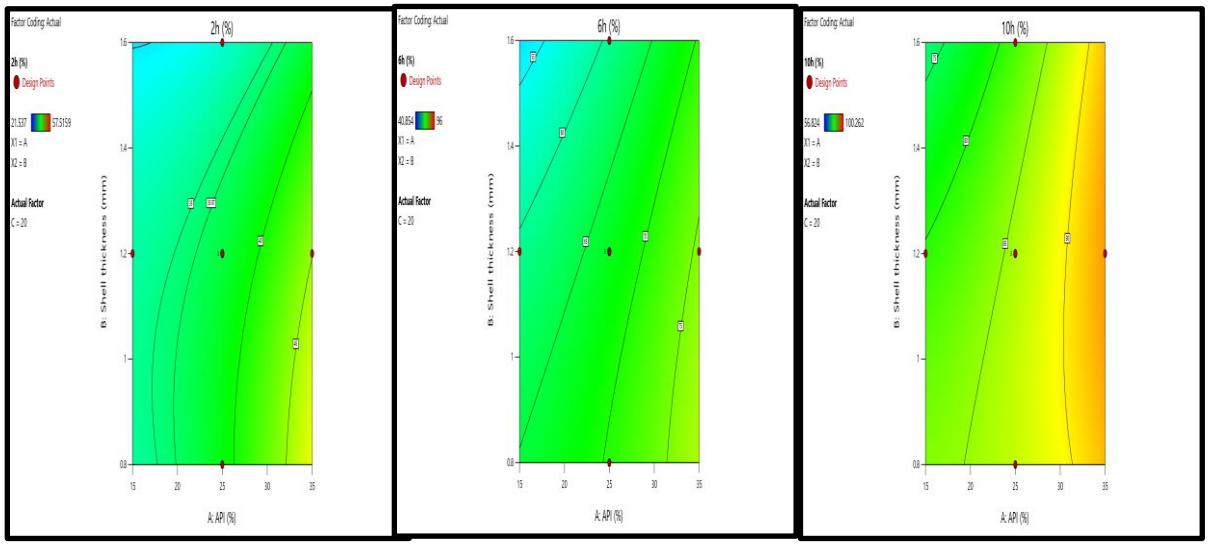

Fig. 4.7. Representative 2D contours describing impact of parameters on drug release

4.4.5.5 Optimization

The developed model was applied to print floating tablets with predetermined target values. The desired target values (responses) were provided to the software (Design-ExpertR version 11) to get the optimized independent variables (predictors). The values of the desired cumulative dissolution values at 2nd, 6th, and 10th hour were provided in Table 5.

Table 4.5. Desired target values predicted and experimental values.

Response	Range	Target	Predicted	Experimental
% release at 2nd h	35-45	40	42.34	40.65
% release at 6th h	65-75	70	75	72.53
% release at 10th h	90-10	90	92.86	95.78

The values of independent of factors provided by the software were used in the preparation of floating tablets (API-35% (w/w), Shell thickness -1.6mm and EC -15% (w/w). The printed tablets

were assessed for in vitro dissolution tests and in vitro floating studies. The printed tablets showed good floating behavior. The in vitro dissolution values were close to the values suggested by the software with less than 5% variance. The experimental values were provided in table 5.

4.4.6 Scanning electron microscopy

The surface of printed floating tablets was observed with scanning electron microscope to see the differences in the surface morphology in the formulations with ethyl cellulose and without ethyl cellulose (Fig. 8). The surface of tablet formulated with ethyl cellulose (b) was rougher compared to tablet without ethyl cellulose (a). This difference in surface morphology can be explained by the reason that EC and HPMC were not homogeneously mixed during HME process and resulted in uneven flow of material from 3D printer nozzle resulting in rougher surface of tablets.

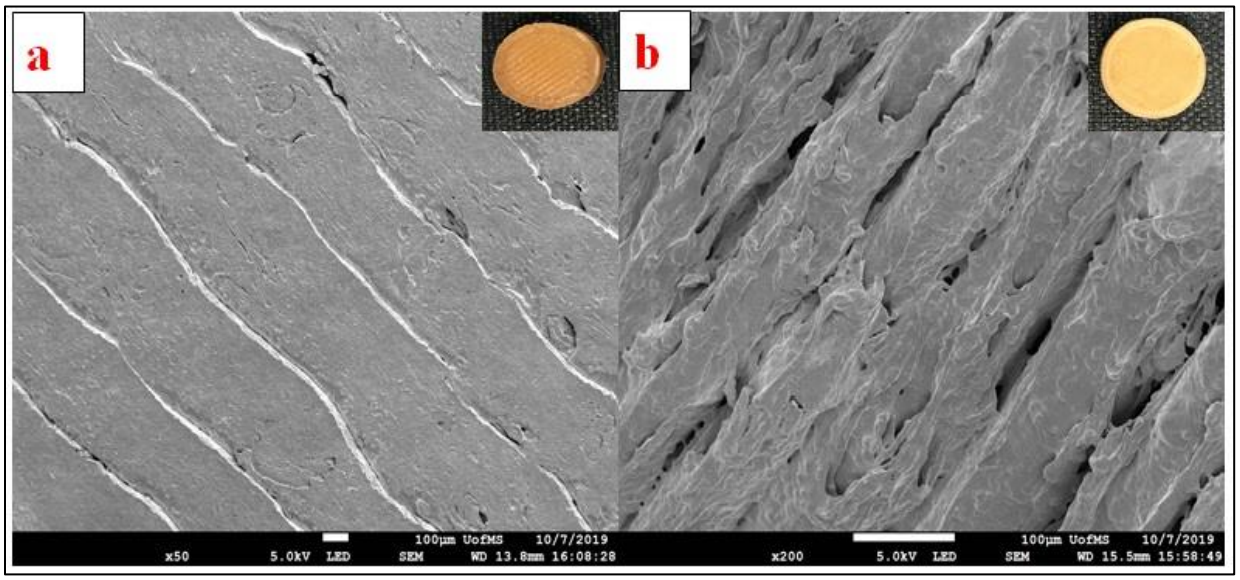

Fig. 4.8. SEM of the 3D printed tablets a) without EC B) with EC

4.5 Conclusions

Filaments suitable for FDM 3D printing were successfully fabricated using different ratios of HPMC, EC and APAP using QbD approach. Sustained release gastroretentive floating tablets were prepared with HME coupled 3D printing. All the three independent factors studied had significant effect on drug release profiles. Both % APAP and % EC were found to be significantly influenced the drug release at 2h, 6h and 10h ($p<0.05$), whereas shell thickness had significant effect at only at 2^{nd} h and 6^{th} h and lost effect at 10th hour ($p=0.0636$). No interaction is seen between all three factors ($p>0.05$), but at 10th hour, when shell thickness lost effect, there is an interaction between drug load and % EC ($p=0.0053$). In conclusion, HME coupled 3D printing is novel viable tool for fabricating customized dosage forms for personalized pharmacotherapy.

BIBLIOGRAPHY

Pinto JF. Site-specific drug delivery systems within the gastro-intestinal tract: from the mouth to the colon. Int J Pharm. 2010;395(1-2):44-52.

T. Bussemer, I. Otto, R. Bodmeier. Pulsatile drug-delivery systems. Crit. Rev. Ther. Drug Carrier Syst., 18 (2001), pp. 433-458

Das S, Deshmukh R, Jha A. Role of natural polymers in the development of multiparticulate systems for colon drug targeting. Syst Rev Pharmacy. 2010;1(1):79–85.

Worsøe, J.; Fynne, L.; Gregersen, T.; Schlageter, V.; Christensen, L.A.; Dahlerup, J.F.; Rijkhoff, N.J.; Laurberg, S.; Krogh, K. Gastric transit and small intestinal transit time and motility assessed by a magnet tracking system. BMC Gastroenterol. 2011.

Streubel, A.; Siepmann, J.; Bodmeier, R. Gastroretentive drug delivery systems. Expert Opin. Drug Deliv. 2006, 3, 217–233.

F. Siepmann, J. Siepmann, M. Walther, R.J. Macrae, R. Bodmeier. Polymer blends for controlled release coatings. J. Control. Rel., 125 (2008), pp. 1-15

Patil H, Tiwari RV, Repka MA. Hot-melt extrusion: from theory to application in pharmaceutical formulation. AAPS PharmSciTech. 2016;17(1):20–42.
S. Das et al.; 2010; J. Worsoe et al., 2011; A. Streubel et al., 2006.

Repka MA, Bandari S, Kallakunta VR, Vo AQ, McFall H, Pimparade MB, et al. Melt extrusion with poorly soluble drugs—an integrated review. Int J Pharm. 2018;535(1–2):68–85.

Tiwari RV, Patil H, Repka MA. Contribution of hot-melt extrusion technology to advance drug delivery in the 21st century. Expert Opin Drug Deliv. 2016;13(3):451–64.

Maniruzzaman M, Boateng JS, Snowden MJ, Douroumis D. A review of hot-melt extrusion: process technology to pharmaceutical products. ISRN Pharm.

H. Sugihara, Y. Matsui, H. Takeuchi, et al. Development of a gastric retentive system as a sustained-release formulation of pranlukast hydrate and its subsequent in vivo verification in human studies. Eur J Pharm Sci, 53 (2014), pp. 62-68.

A.K. Nayak, J. Malakar, K.K. Sen. Gastroretentive drug delivery technologies: current approaches and future potential. J Pharm Educ Res, 1 (2010), pp. 1-12

R.S. Kesarla, P.A. Vora, B.K. Sridhar, et al. Formulation and evaluation of floating tablet of H2-receptor antagonist. Drug Dev Ind Pharm, 41 (2015), pp. 1499-1511.

Lopes CM, Bettencourt C, Rossi A, Buttini F, Barata P. Overview on gastroretentive drug delivery systems for improving drug bioavailability. Int J Pharm. 2016 Aug 20; 510(1):144-58.

Tripathi J, Thapa P, Maharjan R, Jeong SH. Current State and Future Perspectives on Gastroretentive Drug Delivery Systems. Pharmaceutics. 2019;11(4):193. Published 2019 Apr 20. doi:10.3390/pharmaceutics11040193.

Thitinan, S.; McConville, J.T. Development of a gastroretentive pulsatile drug delivery platform. J Pharm Pharmacol. 2012, 64(4), 505-16.

Jain, D.; Raturi, R.; Jain, V.; Bansal, P.; Singh, R. Recent technologies in pulsatile drug delivery systems. Biomatter. 2011, 1(1), 57-65.

Sunil, S.A.; Srikanth, M.V.; Rao, N.S.; Uhumwangho, M.U.; Latha, K.; Murthy, K.V. Chronotherapeutic drug delivery systems: an approach to circadian rhythms diseases. Curr Drug Deliv. 2011, 8(6), 622-33.

Maroni, A.; Zema, L.; Del Curto, M.D.; Loreti, G.; Gazzaniga, A. Oral pulsatile delivery: rationale and chronopharmaceutical formulations. Int J Pharm. 2010, 398(1-2), 1-8.

Almutairy, B.K.; Alshetaili, A.S.; Ashour, E.A.; Patil, H.; Tiwari, R.V.; Alshehri, S.M.; Repka, M.A. Development of a floating drug delivery system with superior buoyancy in gastric fluid using hot-melt extrusion coupled with pressurized CO2. Pharmazie 2016, 71, 128–133.

Trenfield, S.J.; Awad, A.; Goyanes, A.; Gaisford, S.; Basit, A.W. 3D Printing Pharmaceuticals: Drug Development to Frontline Care. Trends Pharmacol. Sci. 2018, 39, 440–451.

Goyanes, A.; Det-Amornrat, U.;Wang, J.; Basit, A.W.; Gaisford, S. 3D scanning and 3D printing as innovative technologies for fabricating personalized topical drug delivery systems. J. Control. Release 2016, 234, 41–48.

Maroni, A.; Melocchi, A.; Parietti, F.; Foppoli, A.; Zema, L.; Gazzaniga, A. 3D printed multi-compartment capsular devices for two-pulse oral drug delivery. J. Control. Release

2017, 268, 10–18.Yang, Y.; Wang, H.; Li, H.; Ou, Z.; Yang, G. 3D printed tablets with internal sca
old structure using ethylcellulose to achieve sustained ibuprofen release. Eur. J. Pharm. Sci. 2018, 115, 11–18.

Chen, D.; Xu, X.Y.; Li, R.; Zhang, G.A.; Zhang, Y.;Wang, M.R.; Xiong, M.F.; Xu, J.R.;Wang, T.; Hu, Q.; et al. Preparation and In vitro Evaluation of FDM 3D-Printed Ellipsoid-Shaped Gastric Floating Tablets with Low infill Percentages. AAPS PharmSciTech 2020, 21, 6.

Thitinan, S; McConville JT. Development of a gastroretentive pulsatile drug delivery platform. J Pharm Pharmacol. 2012, 64(4), 505-16.

Jain, D; Raturi, R; Jain, V; Bansal, P; Singh, R. Recent technologies in pulsatile drug delivery systems. Biomatter. 2011, 1(1), 57-65.

Sunil, SA; Srikanth, MV; Rao, NS; Uhumwangho, MU; Latha, K; Murthy, KV. Chronotherapeutic drug delivery systems: an approach to circadian rhythms diseases. Curr Drug Deliv. 2011, 8(6), 622-33.

Streubel, A; Siepmann, J; Bodmeier, R. Gastroretentive drug delivery systems. Expert Opin Drug Deliv. 2006, 3(2), 217-33.

Worsøe, J; Fynne, L; Gregersen, T; Schlageter, V; Christensen, LA,; Dahlerup, JF; Rijkhoff, NJ; Laurberg, S; Krogh, K. Gastric transit and small intestinal transit time and motility assessed by a magnet tracking system. BMC Gastroenterol. 2011, 11, 145.

Md. Lutful Amin, * Tajnin Ahmed, and Md. Abdul Mannan. Development of Floating-Mucoadhesive Microsphere for Site Specific Release of Metronidazole. Adv Pharm Bull. 2016 Jun; 6(2): 195–200.

Preda M1, Leucuta SE. Oxprenolol-loaded bioadhesive microspheres: preparation and in vitro/in vivo characterization. J Microencapsul. 2003 Nov-Dec;20(6):777-89.
Garg R., Gupta G. Progress in controlled gastroretentive delivery systems. Trop. J. Pharm. Res. 2008; 7:1055–1066.

Chen J1, Park H, Park K. Synthesis of superporous hydrogels: hydrogels with fast swelling and superabsorbent properties. J Biomed Mater Res. 1999 Jan;44(1):53-62.

Almutairy BK, Alshetaili AS, Ashour EA, Patil H, Tiwari RV, Alshehri SM, Repka MA. Development of a floating drug delivery system with superior buoyancy in gastric fluid using hot-melt extrusion coupled with pressurized CO_2. Pharmazie. 2016 Mar;71(3):128-33.

Reddy, AB; Reddy, ND. Development of Multiple-Unit Floating Drug Delivery System of Clarithromycin: Formulation, in vitro Dissolution by Modified Dissolution Apparatus, in vivo Radiographic Studies in Human Volunteers. Drug Res (Stuttg). 2017, 67(7), 412-418.

Lalge R, Thipsay P, Shankar VK, Maurya A, Pimparade M, Bandari S, Zhang F, Murthy SN3, Repka MA4. Preparation and evaluation of cefuroxime axetil gastro-retentive floating drug delivery system via hot melt extrusion technology. Int J Pharm. 2019 Jul 20;566:520-531.

Vo AQ, Feng X, Morott JT1, Pimparade MB1, Tiwari RV1, Zhang F2, Repka MA3. A novel floating controlled release drug delivery system prepared by hot-melt extrusion. Eur J Pharm Biopharm. 2016 Jan;98:108-21. doi: 10.1016/j.ejpb.2015.11.015. Epub 2015 Nov 28.

He W., Li Y., Zhang R., Wu Z., Yin L. Gastro-floating bilayer tablets for the sustained release of metformin and immediate release of pioglitazone: Preparation and in vitro/in vivo evaluation. Int. J. Pharm. 2014; 476:223–231.

Tiwari RV1, Patil H1, Repka MA1,2. Contribution of hot-melt extrusion technology to advance drug delivery in the 21st century. Expert Opin Drug Deliv. 2016;13(3):451-64.

Pimparade MB1, Morott JT1, Park JB2, Kulkarni VI1, Majumdar S3, Murthy SN1, Lian Z4, Pinto E4, Bi V4, Durig T4, Murthy R5, Shivakumar HN5, Vanaja K6, Kumar PC6, Repka MA7. Development of taste masked caffeine citrate formulations utilizing hot melt extrusion technology and in vitro-in vivo evaluations. Int J Pharm. 2015 Jun 20;487(1-2):167-76.

Sindhuri Maddineni, Sunil Kumar Battu, Joe Morott, Soumyajit Majumdar, and Michael A. Repka1,2, Formulation Optimization of Hot Melt. Extruded Abuse Deterrent Pellet Dosage Form Utilizing Design of Experiments (DOE). J Pharm Pharmacol. 2014 Feb; 66(2): 309–322.

Lakshman JP1, Cao Y, Kowalski J, Serajuddin AT. Application of melt extrusion in the development of a physically and chemically stable high-energy amorphous solid dispersion of a poorly water-soluble drug. Mol Pharm. 2008 Nov-Dec;5(6):994-1002.

Bhagurkar AM1, Angamuthu M1, Patil H1, Tiwari RV1, Maurya A1, Hashemnejad SM2, Kundu S2, Murthy SN1, Repka MA3,4. Development of an Ointment Formulation Using Hot-Melt Extrusion Technology. AAPS PharmSciTech. 2016 Feb;17(1):158-66.

Dumpa NR1, Sarabu S1, Bandari S1, Zhang F2, Repka MA3. Chronotherapeutic Drug Delivery of Ketoprofen and Ibuprofen for Improved Treatment of Early Morning Stiffness

in Arthritis Using Hot-Melt Extrusion Technology. AAPS PharmSciTech. 2018 Aug;19(6):2700-2709.

Goole J1, Amighi K2. 3D printing in pharmaceutics: A new tool for designing customized drug delivery systems. Int J Pharm. 2016 Feb 29;499(1-2):376-394. doi: 10.1016/j.ijpharm.2015.12.071. Epub 2016 Jan 3.

Trenfield SJ1, Awad A1, Goyanes A2, Gaisford S3, Basit AW4. 3D Printing Pharmaceuticals: Drug Development to Frontline Care. Trends Pharmacol Sci. 2018 May;39(5):440-451. doi: 10.1016/j.tips.2018.02.006. Epub 2018 Mar 11.

J1, Yu X2, Jin Y3. 3D printing of vaginal rings with personalized shapes for controlled release of progesterone. Int J Pharm. 2018 Mar 25;539(1-2):75-82.
Sadia M1, Arafat B2, Ahmed W3, Forbes RT1, Alhnan MA4. Channelled tablets: An innovative approach to accelerating drug release from 3D printed tablets. J Control Release. 2018 Jan 10;269:355-363.

Kun Liang,* Simone Carmone, Davide Brambilla,† and Jean-Christophe Leroux‡ 3D printing of a wearable personalized oral delivery device: A first-in-human study. Sci Adv. 2018 May; 4(5).

Goyanes A1, Det-Amornrat U1, Wang J1, Basit AW2, Gaisford S3. 3D scanning and 3D printing as innovative technologies for fabricating personalized topical drug delivery systems. J Control Release. 2016 Jul 28; 234:41-8.

Chai, X., Chai, H., Wang, X., Yang, J., Li, J., Zhao, Y., Cai, W., Tao, T., & Xiang, X. (2017). Fused Deposition Modeling (FDM) 3D Printed Tablets for Intragastric Floating Delivery of Domperidone. Scientific Reports

Li Q1, Guan X2, Cui M1, Zhu Z1, Chen K1, Wen H1, Jia D3, Hou J4, Xu W4, Yang X5, Pan W6. Preparation and investigation of novel gastro-floating tablets with 3D extrusion-based printing. Int J Pharm. 2018 Jan 15;535(1-2):325-332.

Maroni A1, Melocchi A2, Parietti F3, Foppoli A1, Zema L4, Gazzaniga A1. 3D printed multi-compartment capsular devices for two-pulse oral drug delivery. J Control Release. 2017 Dec 28;268:10-18.

Zhang J1, Yang W2, Vo AQ1, Feng X1, Ye X1, Kim DW1, Repka MA3. Hydroxypropyl methylcellulose-based controlled release dosage by melt extrusion and 3D printing: Structure and drug release correlation. Carbohydrate Polym. 2017 Dec 1;177:49-57.

Yang Y1, Wang H1, Li H1, Ou Z1, Yang G2. 3D printed tablets with internal scaffold structure using ethyl cellulose to achieve sustained ibuprofen release. Eur J Pharm Sci. 2018 Mar 30;115:11-18.
Korte C1, Quodbach J2. 3D-Printed Network Structures as Controlled-Release Drug Delivery Systems: Dose Adjustment, API Release Analysis and Prediction. AAPS PharmSciTech. 2018 Nov;19(8):3333-3342.

Khan Z, Pillay V, Choonara YE, Du Toit LC. Drug delivery technologies for chronotherapeutic applications. Pharm Dev Technol. 2009;14(6):602-12.

Mandal AS, Biswas N, Karim KM, Guha A, Chatterjee S, Behera M, Kuotsu K. Drug delivery system based on chronobiology--A review. J Control Release. 2010;147(3):314-25.
Saitoh T, Watanabe Y, Kubo Y, et al. Intragastric acidity and circadian rhythm. Biomed Pharmacother. 2001; 55:138-141.

Roy P, Shahiwala A. Statistical optimization of ranitidine HCl floating pulsatile delivery system for chronotherapy of nocturnal acid breakthrough. Eur J Pharm Sci. 2009 Jun 28;37(3-4):363-9.

Nayak UY, Shavi GV, Nayak Y, et al. Chronotherapeutic drug delivery for early morning surge in blood pressure: a programmable delivery system. J Control Release. 2009;136(2):125-31.

Jose S, Prema MT, Chacko AJ, Thomas AC, Souto EB. Colon specific chitosan microspheres for chronotherapy of chronic stable angina. Colloids Surf B Biointerfaces. 2011;83(2):277-83.

Shiohira H, Fujii M, Koizumi N, Kondoh M, Watanabe Y. Novel chronotherapeutic rectal aminophylline delivery system for therapy of asthma. Int J Pharm. 2009;379(1):119-24.

Wang H, Cheng L, Wen H, et al. A time-adjustable pulsatile release system for ketoprofen: In vitro and in vivo investigation in a pharmacokinetic study and an IVIVC evaluation. Eur J Pharm Biopharm. 2017;119:192-200.

Repka MA, Bandari S, Kallakunta VR, et al. Melt extrusion with poorly soluble drugs - An integrated review. Int J Pharm. 2018;535(1-2):68-85.

Patil H, Tiwari RV, Repka MA. Hot-Melt Extrusion: from Theory to Application in Pharmaceutical Formulation. AAPS PharmSciTech. 2016;17(1):20-42.

Tiwari RV, Patil H, Repka MA. Contribution of hot-melt extrusion technology to advance drug delivery in the 21st century. Expert Opin Drug Deliv. 2016;13(3):451-64.

De Jaeghere W, De Beer T, Van Bocxlaer J, Remon JP1, Vervaet C. Hot-melt extrusion of polyvinyl alcohol for oral immediate release applications. Int J Pharm. 2015;492(1-2):1-9.

Puri V, Brancazio D, Desai PM, et al. Development of Maltodextrin-Based Immediate-Release Tablets Using an Integrated Twin-Screw Hot-Melt Extrusion and Injection-Molding Continuous Manufacturing Process. J Pharm Sci. 2017;106(11):3328-3336.

Mohammed NN, Majumdar S, Singh A, et al. Klucel™ EF and ELF polymers for immediate-release oral dosage forms prepared by melt extrusion technology. AAPS PharmSciTech. 2012;13(4):1158-69.

Verstraete G, Van RJ, Van Bockstal PJ, et al. Hydrophilic thermoplastic polyurethanes for the manufacturing of highly dosed oral sustained release matrices via hot melt extrusion and injection molding. Int J Pharm. 2016;506(1-2):214-21.

Patil H, Tiwari RV, Upadhye SB, Vladyka RS, Repka MA. Formulation and development of pH-independent/dependent sustained release matrix tablets of ondansetron HCl by a continuous twin-screw melt granulation process. Int J Pharm. 2015;496(1):33-41.

Repka MA, McGinity JW. Influence of vitamin E TPGS on the properties of hydrophilic films produced by hot-melt extrusion. Int J Pharm. 2000;202(1-2):63-70.

Bhagurkar AM, Angamuthu M, Patil H, et al. Development of an Ointment Formulation Using Hot-Melt Extrusion Technology. AAPS PharmSciTech. 2016;17(1):158-66.

Mendonsa NS, Thipsay P, Kim DW, Martin ST, Repka MA. Bioadhesive Drug Delivery System for Enhancing the Permeability of a BCS Class III Drug via Hot-Melt Extrusion Technology. AAPS PharmSciTech. 2017;18(7):2639-2647.

Palem CR1, Kumar Battu S, Maddineni S, Gannu R, Repka MA, Yamsani MR. Oral transmucosal delivery of domperidone from immediate release films produced via hot-melt extrusion technology. Pharm Dev Technol. 2013;18(1):186-95.

Patil H, Kulkarni V, Majumdar S, Repka MA. Continuous manufacturing of solid lipid nanoparticles by hot melt extrusion. Int J Pharm. 2014;471(1-2):153-6.

Ye X, Patil H, Feng X, et al. Conjugation of Hot-Melt Extrusion with High-Pressure Homogenization: A Novel Method of Continuously Preparing Nanocrystal Solid Dispersions. AAPS PharmSciTech. 2016;17(1):78-88.

Bruce LD, Shah NH, Malick AW, Infeld MH, McGinity JW. Properties of hot-melt extruded tablet formulations for the colonic delivery of 5-aminosalicylic acid. Eur J Pharm Biopharm. 2005;59(1):85-97.

Mehuys E, Remon JP, Vervaet C. Production of enteric capsules by means of hot-melt extrusion. Eur J Pharm Sci. 2005;24(2-3):207-12.

Castellsague J, Riera-Guardia N, Calingaert B, et al. Individual NSAIDs and upper gastrointestinal complications: a systematic review and meta-analysis of observational studies. Drug Saf. 2012;35(12):1127-46.

S, Yang LP. Modified-release prednisone: in patients with rheumatoid arthritis. Drugs. 2013;73(18):2067-76.

Pozzi P, Furlani A, Gazzanig, Davis S.S, Wilding IR. The time clock system: a new oral dosage form for fast and complete release of drug after a predetermined lag time. J Control Release. 1994;31(1):99-108.

Yang R, Wang Y, Zheng X, Meng J, Tang X, Zhang X. Preparation, and evaluation of ketoprofen hot-melt extruded enteric and sustained-release tablets. Drug Dev Ind Pharm. 2008;34(1):83-9.

Schilling SU, Shah NH, Waseem Malick A, McGinity JW. Properties of melt extruded enteric matrix pellets. Eur J Pharm Biopharm. 2010;74(2):352-61.

Andrews GP, Jones DS, Diak OA, McCoy CP, Watts AB, McGinity JW. The manufacture and characterisation of hot melt extruded enteric tablets. Eur J Pharm Biopharm. 2008;69(1):264-73.

Kalivoda A, Fischbach M, Kleinebudde P. Application of mixtures of polymeric carriers for dissolution enhancement of fenofibrate using hot-melt extrusion. Int J Pharm. 2012;429(1-2):58-68.

Dokoumetzidis A, Macheras P. A century of dissolution research: from Noyes and Whitney to the biopharmaceutics classification system. Int J Pharm. 2006 Sep 14;321(1-2):1-11.

Zhang F. Melt-Extruded Eudragit® FS-Based Granules for Colonic Drug Delivery. AAPS PharmSciTech. 2016 Feb;17(1):56-67.

VITA

NAGIREDDY DUMPA

Contact no:| (662)-638-5041| nagireddy.dumpa@gmail.com

December 2016	Pharm. D (Doctor of Pharmacy) C.L. Baid Metha College of Pharmacy, India
May 2021	Doctor of Philosophy (Ph. D) in Pharmaceutics and Drug Delivery University of Mississippi, Oxford, MS
Peer reviewed publications	10

Professional activities

1. Reviewer	AAPS Phamrascitech JDDST DDIP
2. Member	Rho Chi
3. Instructor	Hands on tablet course